



Research paper

Structure-based discovery of novel 4-(2-fluorophenoxy)quinoline derivatives as c-Met inhibitors using isocyanide-involved multicomponent reactions

Xiang Nan ^a, Hui-Jing Li ^{a, b, **}, Sen-Biao Fang ^{c, ***}, Qin-Ying Li ^{a, b}, Yan-Chao Wu ^{a, b, *}^a School of Marine Science and Technology, Harbin Institute of Technology, Weihai, 264209, PR China^b Weihai Institute of Marine Biomedical Industrial Technology, Wendeng District, Weihai, 264400, PR China^c School of Computer Science and Engineering, Central South University, Changsha, 410082, PR China

ARTICLE INFO

Article history:

Received 31 January 2020

Received in revised form

1 March 2020

Accepted 13 March 2020

Available online 16 March 2020

Keywords:

4-(2-fluorophenoxy)quinoline derivatives
c-Met inhibitors
Isocyanide-involved multicomponent
reactions
Biological evaluation
Docking study

ABSTRACT

The c-Met kinase has emerged as a promising target for the development of small molecule antitumor agents because of its close relationship with the progression of many human cancers, poor clinical outcomes and even drug resistance. In this study, two novel series of 6,7-disubstituted-4-(2-fluorophenoxy)quinoline derivatives containing α -acyloxycarboxamide or α -acylaminoamide scaffolds were designed, synthesized, and evaluated for their *in vitro* biological activities against c-Met kinase and four cancer cell lines (H460, HT-29, MKN-45, and MDA-MB-231). Most of the target compounds exhibited moderate to significant potency and possessed selectivity for H460 and HT-29 cancer cell lines. The preliminary structure-activity relationships indicated that α -acyloxycarboxamide or α -acylaminoamide as 5-atom linker contributed to the antitumor potency. Among these compounds, compound **10m** (c-Met IC₅₀ = 2.43 nM, a multitarget tyrosine kinase inhibitor) exhibited the most potent inhibitory activities against H460, HT-29 and MDA-MB-231 cell lines with IC₅₀ of 0.14 ± 0.03 μ M, 0.20 ± 0.02 μ M and 0.42 ± 0.03 μ M, which were 1.7-, 1.3- and 1.6-fold more active than foretinib, respectively. In addition, concentration-dependent assay and time-dependent assay indicated compound **10m** can inhibit the proliferation of H460 cell in a time and concentration dependent manner. Moreover, docking studies revealed the common mode of interaction with the c-Met binding site, suggesting that **10m** is a potential candidate for cancer therapy deserving further study.

© 2020 Elsevier Masson SAS. All rights reserved.

1. Introduction

Mesenchymal–epithelial transition factor (c-Met) is a prototype member of a heterodimeric receptor tyrosine kinase subfamily and the only known high-affinity receptor for hepatocyte growth factor/scatter factor (HGF/SF) [1,2]. The HGF/c-Met signaling has been identified to play a vital role in many normal physiological processes (Fig. 1), such as mitogenesis, motogenesis and morphogenesis, by activating multiple downstream signal transduction

pathways, including Ras/MEK/MAPK, PI3K/AKT and Ras/RAC1/PAK pathways [3–5]. However, HGF/c-Met axis deregulation through constitutive activation, gene amplification, mutations, and activation of an autocrine loop plays a key role in numerous malignancies and promotes tumor growth, invasion, dissemination and/or angiogenesis [6–12]. Additionally, dysregulated HGF/c-Met signaling has been also associated with poor clinical outcomes and resistance acquisition to some approved targeted therapies [13–17]. Thus, c-Met has attracted consistent interest as a potential target for cancer drug discovery. As c-Met tyrosine kinase inhibitors (TKIs) are believed to be effective for both ligand-dependent and independent activation of c-Met, they are the most attractive methods for targeting the c-Met pathway, and have made a respectable number of c-Met TKIs into clinical trials or approved as anticancer drugs [18–20]. In general, the c-Met TKIs can be categorized into two types based on the chemical types and different binding modes of the DFG motif of the c-Met activation loop

* Corresponding author. School of Marine Science and Technology, Harbin Institute of Technology, Weihai, 264209, PR China.

** Corresponding author. School of Marine Science and Technology, Harbin Institute of Technology, Weihai, 264209, PR China.

*** Corresponding author.

E-mail addresses: lihuiping@iccas.ac.cn (H.-J. Li), fangsb@csu.edu.cn (S.-B. Fang), ycwu@iccas.ac.cn (Y.-C. Wu).

[21–26], and **Type II** inhibitors may be more effective than **Type I** inhibitors against the mutations near the active site of c-Met [27–33]. This is because **Type II** inhibitors not only bind to the same area occupied by the **Type I** inhibitors, but also utilize the hydrogen bonding and hydrophobic interaction with the allosteric site, which is beyond the entrance of the c-Met active site.

Accordingly, various **Type II** c-Met inhibitors have been developed, amongst which 6,7-disubstituted-4-(2-fluorophenoxy)quinolines are drawing the most attention. Many of these derivatives are under clinical or preclinical research, such as cabozantinib, Kirin Brewery, Amgen, MG10, MethylGene and foretinib [34–38]. As shown in Fig. 2, the structure-activity relationships of quinoline-based inhibitors disclosed that 6,7-disubstituted-4-phenoxyquinoline framework (moiety A) and an aryl fragment (moiety B) should be preserved as the privileged scaffolds in that the quinoline core formed hydrogen bonds and maintained vander Waals interactions with the backbone of c-Met kinase, and the moiety B probably fitted into the hydrophobic pocket [39–42]. More importantly, these 6,7-disubstituted-4-phenoxyquinoline derivatives have two common structural features in their linkers between moiety A and moiety B which is known as '**5 atoms regulation/hydrogen-bond donors or acceptors**' [43–47]. These structural characteristics suggested that the exploration of a suitable linker might be a feasible way to discover new quinoline-based **Type II** c-Met inhibitors.

Although many endeavors have been paid to the construction of the 5-atom linker, one-step synthesis of the 5-atom linker is still a significant challenge. The multi-step synthetic strategies put preparation of sufficient quantities of quinoline-based **Type II** c-Met inhibitors for biological evaluation and medical studies at a

disadvantage. Thus, the development of a new protocol for the facile synthesis of the 5-atom linker becomes a high priority. Multicomponent reactions (MCRs) [48–53] deemed to satisfy this criterion due to their utility in rapid construction of structurally diverse, complex, and chemical libraries of "drug-like" molecules from simple precursors [54–56]. In particular, MCRs that involve isocyanides (IMCRs) are by far the most versatile reactions in terms of scaffolds and number of accessible compounds, and they form the basis of the well-known Passerini and Ugi reactions [57–59]. Passerini and Ugi reactions could provide one-pot synthesis of α -acyloxy carboxamide and α -acyl aminoamide fragments, respectively. Inspiringly, the α -acyloxy carboxamide and α -acyl aminoamide framework conformed to the characteristic of the '**5 atoms regulation**' and contained both **hydrogen-bond donor and acceptor**, indicating that they could be the suitable linkers mentioned above. In addition, compounds bearing α -acyloxy carboxamide or α -acyl aminoamide scaffold have been reported to exhibit a broad spectrum of biological activities (Fig. 3), including antitumor, antiinflammatory, antimarial and antituberculosis, etc [60,61]. Accordingly, we envisioned that the utilization of IMCRs (Passerini and Ugi reactions) would provide a rapid and effective synthetic way for the construction of the suitable 5-atom linkers, thus facilitating the discovery of new c-Met inhibitors [62,63]. Herein, we first report the use of Passerini (P-3CR) and Ugi (Ugi-4CR) reactions as a versatile approach towards the synthesis of 6,7-disubstituted-4-phenoxyquinoline derivatives that bearing α -acyloxy carboxamide and α -acyl aminoamide, respectively. Meanwhile, various substituents were introduced into the moiety B as well as the 5-atom linkers to investigate their effects on activity. All target compounds were evaluated for their c-Met kinase activity and

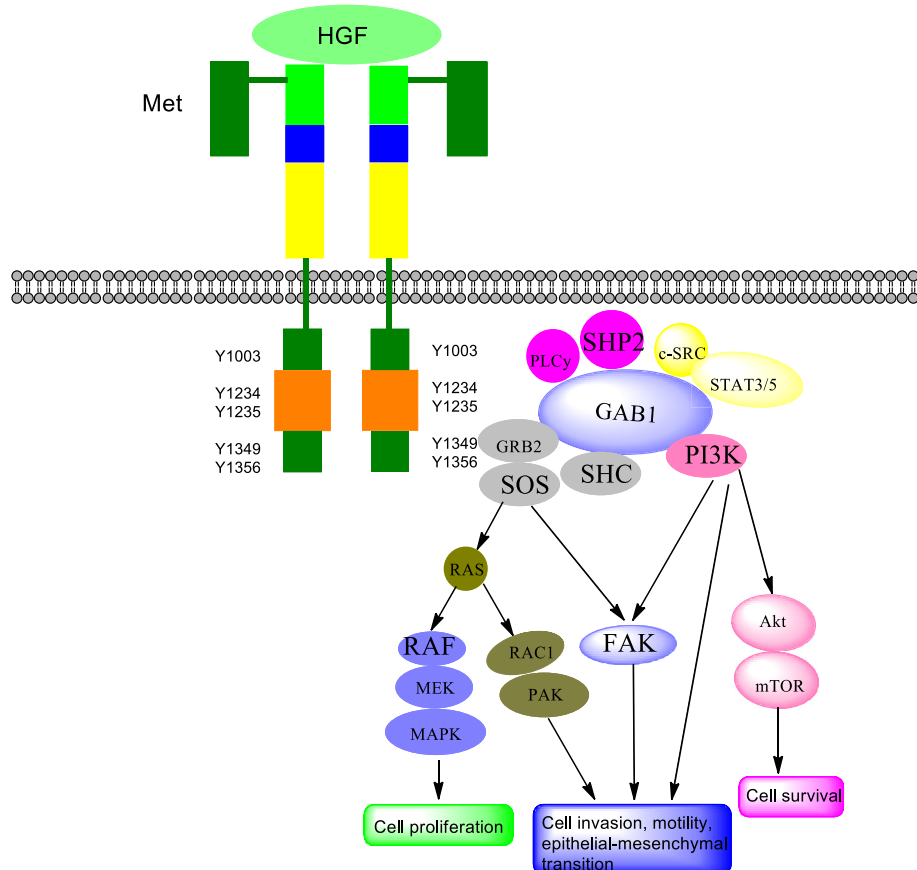


Fig. 1. The signaling pathways of c-Met.

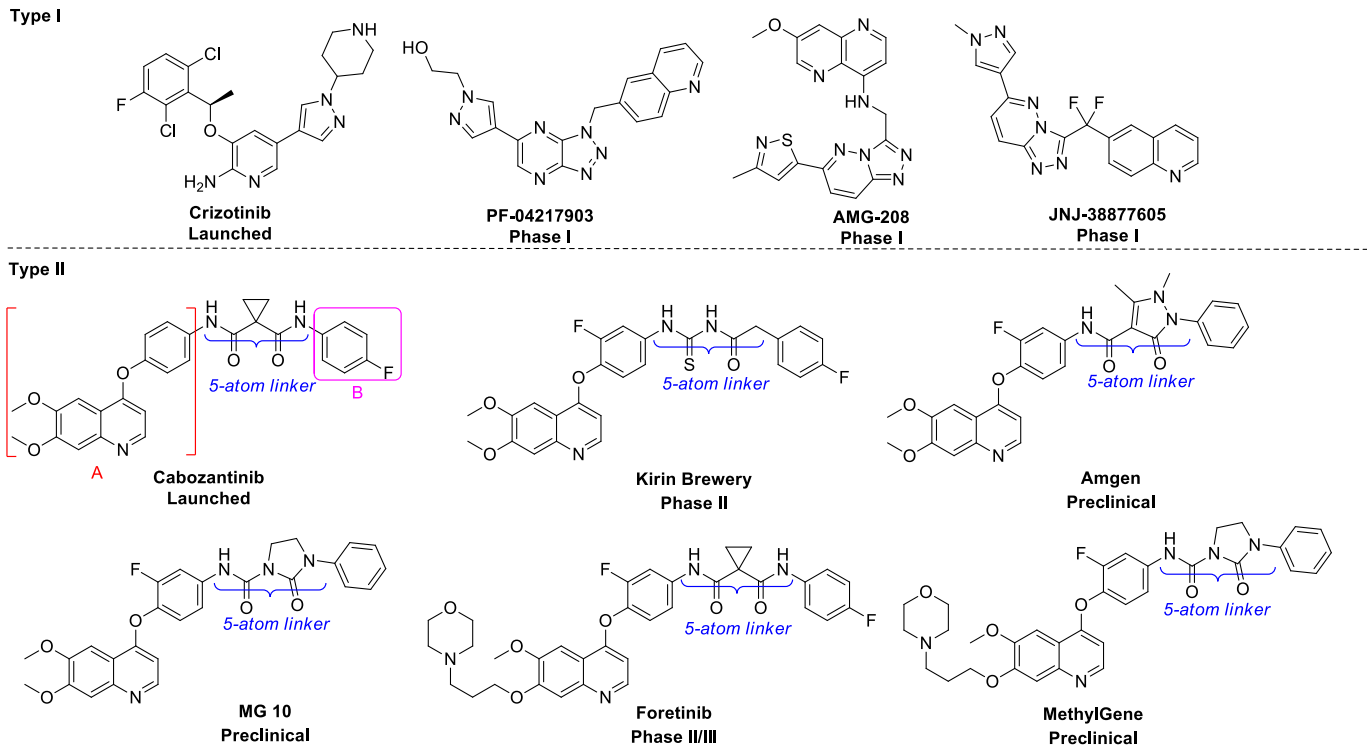


Fig. 2. The representative c-Met kinase inhibitors of different types.

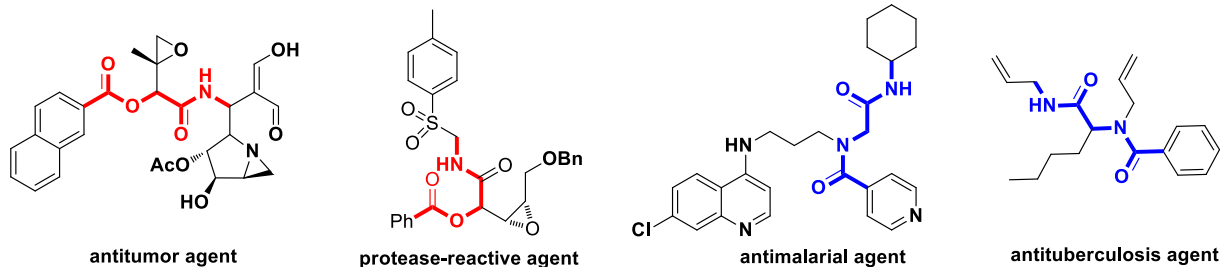


Fig. 3. Structures of α -acyloxycarboxamide/ α -acylaminoamide and its mimics.

antiproliferative activities against four cancer cell lines, including H460, HT-29, MKN-45 and MDA-MB-231. Subsequently, the kinase selectivity and docking study of the representative compound **10m** was further explored.

2. Results and discussion

2.1. Chemistry

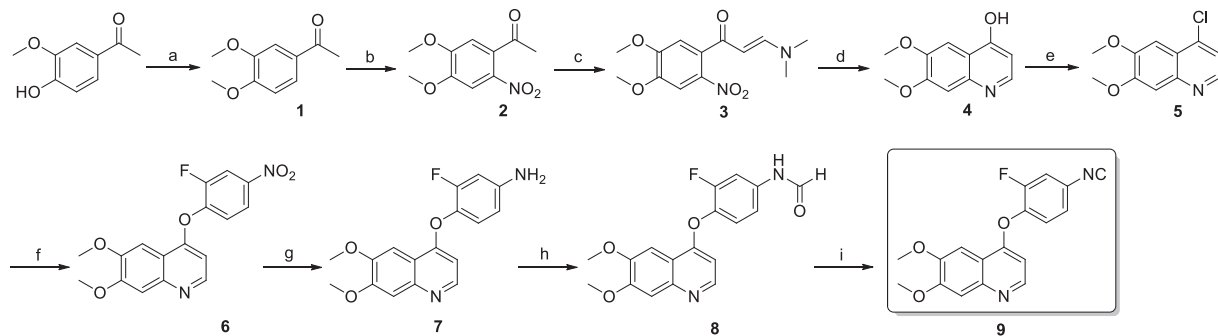
2.1.1. Synthesis of 3-fluoro-4-(6,7-dimethoxyquinolin-4-yloxy)phenylisocyanide (**9**)

As shown in [Scheme 1](#), 3-fluoro-4-(6,7-dimethoxyquinolin-4-yloxy)phenylisocyanide **9** was synthesized from readily available 4-hydroxy-3-methoxy-acetophenone. 4-Hydroxy-3-methoxy-acetophenone was alkylated with iodomethane under basic reaction conditions to afford disubstituted acetophenone **1** in 91% yield. Regioselective nitration of disubstituted acetophenone **1** and subsequent aminomethylation with *N,N*-dimethylformamide dimethyl acetal (DMF-DMA) provided 3-(dimethylamino)-prop-2-en-1-one **3** [64], which underwent an intramolecular cyclization

in the presence of iron powder and acetic acid to afford the desired 4-quinolin-ol **4**. 4-Chloro-quinoline **5** was obtained in 83% yield just by treating 4-quinolin-ol **4** on exposure of phosphorus oxychloride [65]. Subsequently, 4-chloro-quinoline **5** was etherified with 2-fluoro-4-nitrophenol to give nitro **6**, which was then reduced by treating with $\text{SnCl}_2 \cdot 2\text{H}_2\text{O}$ in ethanol to give amide **7** in 36% overall yield [66]. Compound **7** was converted to formamide **8** in 76% yield by reaction with ethyl formate under reflux. Finally, the dehydration of **8**, after the optimization of reaction conditions ([Table 1](#)), was accomplished by treating with phosphorus oxychloride at room temperature in the presence of triethylamine in chloroform to afford the key intermediate isocyanide **9** in 92% yield [67].

2.1.2. Synthesis of the target compounds of α -acyloxycarboxamide/ α -acylaminoamide-based 6,7-dimethoxy-4-(2-fluorophenoxy)quinoline

Two novel series of target compounds **10a–y** and **11a–g** were obtained in moderate to excellent yields via Passerini and Ugi reactions, respectively [68]. The Passerini reaction ([Scheme 2](#))



Scheme 1. Reagents and conditions: (a) CH_3I , K_2CO_3 , acetone, r.t., 4 h; (b) concentrated nitric acid, 0°C , overnight; (c) DMF-DMA, toluene, reflux; (d) Fe (powder), AcOH , 80°C , 2 h; (e) POCl_3 , reflux, DMF (cat.); (f) 2-fluoro-4-nitrophenol, PhCl , 140°C , 20 h; (g) $\text{SnCl}_2 \cdot 2\text{H}_2\text{O}$, EtOH , 70°C , 6 h; (h) ethyl formate, TEA, refluxing, 18 h; (i) POCl_3 , TEA, CHCl_3 , 0°C .

Table 1

Optimization of the reaction conditions for the dehydration of formamide **8**.

Entry	Dehydrant/base	Solvent	Temp ($^\circ\text{C}$)	Yield (%)
1	$\text{PhSO}_2\text{Cl}/\text{C}_5\text{H}_5\text{N}$	$\text{C}_5\text{H}_5\text{N}$	rt	trace
2	$\text{Ph}_3\text{P}/\text{Et}_3\text{N}$	CCl_4	rt	18
3	$\text{Ph}_3\text{P}/\text{Et}_3\text{N}$	CCl_4	40	22
4	$\text{SOCl}_2/\text{Na}_2\text{CO}_3$	DMF	0	26
5	Cyanuric/ Et_3N	CH_2Cl_2	45	35
6	$\text{EtOPtOCl}_2/\text{Et}_3\text{N}$	CH_2Cl_2	45	28
7	$\text{POCl}_3/\text{C}_5\text{H}_5\text{N}$	CHCl_3	0	54
8	$\text{POCl}_3/\text{Et}_3\text{N}$	CHCl_3	0	74
9	$\text{POCl}_3/\text{Et}_3\text{N}$	CHCl_3	rt	92

involved three components: aldehyde/ketone, carboxylic acid, and isocyanide **9**. The reaction gave a series of novel 6,7-dimethoxy-4-(2-fluorophenoxy)quinoline derivatives with an α -acyloxycarboxamide group. The Ugi reaction (Scheme 2) involved four components: aldehyde, amine, carboxylic acid, and isocyanide **9**. This reaction mixture afforded another series of 6,7-dimethoxy-4-(2-fluorophenoxy)quinoline derivatives with a α -acylaminocarboxamide group. All newly synthesized compounds were purified by column chromatography and their structures were characterized by NMR and MS.

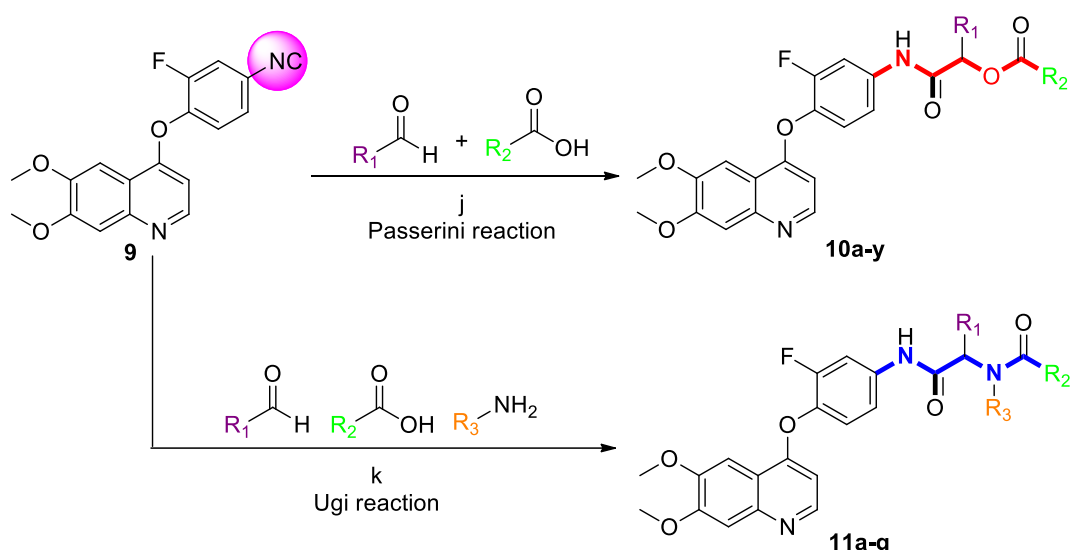
2.2. Biological evaluation

2.2.1. In vitro enzymatic assays and structure-activity relationships

The c-Met enzymatic assays of all newly prepared target compounds were evaluated *in vitro* using homogeneous time-resolved fluorescence (HTRF) assay, taking foretinib as a positive control. The results expressed as the half-maximal inhibitory concentration (IC_{50}) values presented in Table 2, as mean values of experiments performed in triplicate.

As illustrated in Table 2, these novel 6,7-dimethoxy-4-(2-fluorophenoxy)quinoline derivatives bearing α -acyloxycarboxamide/ α -acylaminocarboxamide group were found to be active against c-Met kinase with IC_{50} values ranging from 2.43 to 66.54 nM; three of them (**10m**, $\text{IC}_{50} = 2.43$ nM; **10n**, $\text{IC}_{50} = 4.72$ nM; **10o**, $\text{IC}_{50} = 3.13$ nM) showed comparable potency with foretinib ($\text{IC}_{50} = 1.75$ nM), indicating that the introduction of the new moiety α -acyloxycarboxamide or α -acylaminocarboxamide as ‘five-atom linker’ to 6,7-dimethoxy-4-(2-fluorophenoxy)quinoline framework maintained the potent c-Met kinase inhibitory efficacy. The α -acyloxycarboxamide-contained target compounds **10a-y** exhibited relatively higher c-Met kinase inhibitory efficacy in comparison with α -acylaminocarboxamide-contained target compounds **11a-g**.

As seen from the data in Table 2, compound **10h** ($\text{IC}_{50} = 8.35$ nM; $\text{R}_1 = t\text{-Butyl}$, $\text{R}_2 = \text{Phenyl}$) possessed greater potency than compound **10d** ($\text{IC}_{50} = 22.74$ nM; $\text{R}_1 = \text{Methyl}$, $\text{R}_2 = \text{Phenyl}$), compound



Scheme 2. Reagents and conditions: (j) $\text{THF}/\text{H}_2\text{O} = 3:1$, 0.4 M, 40°C , 24 h; (k) MeOH , 0.2 M, 60°C , 24 h.

Table 2c-Met kinase activities of the target compounds **10a-y** and **11a-g**.

Compd.	R ₁	R ₂	R ₃	C-Met IC ₅₀ (nM)
10a	Methyl	Cyclopentyl	/	52.86 ± 3.48
10b	Methyl	2-Thienyl	/	37.46 ± 4.27
10c	Methyl	2-Naphthyl	/	48.36 ± 3.25
10d	Methyl	Ph	/	22.74 ± 1.58
10e	n-Propyl	Ph	/	19.45 ± 1.90
10f	Cyclohexyl	Ph	/	30.38 ± 2.56
10g	Phenyl	Ph	/	54.42 ± 4.65
10h	t-Butyl	Ph	/	8.35 ± 0.82
10i	t-Butyl	4-Me-Ph	/	12.35 ± 0.94
10j	t-Butyl	4-OMe-Ph	/	21.48 ± 1.65
10k	t-Butyl	3,4,5-(OMe) ₃ -Ph	/	35.64 ± 3.86
10l	t-Butyl	4-(t-Butyl)-Ph	/	18.45 ± 1.35
10m	t-Butyl	4-F-Ph	/	2.43 ± 0.31
(R)- 10m	t-Butyl	4-F-Ph	/	2.56 ± 0.28
(S)- 10m	t-Butyl	4-F-Ph	/	2.49 ± 0.19
10n	t-Butyl	3-F-Ph	/	4.72 ± 0.52
10o	t-Butyl	2-F-Ph	/	3.13 ± 0.42
10p	t-Butyl	4-Cl-Ph	/	7.43 ± 1.16
10q	t-Butyl	3-Cl-Ph	/	7.86 ± 0.92
10r	t-Butyl	2-Cl-Ph	/	8.12 ± 0.85
10s	t-Butyl	4-Br-Ph	/	18.44 ± 2.63
10t	t-Butyl	4-CF ₃ -Ph	/	36.62 ± 2.46
10u	t-Butyl	3,4-(Cl) ₂ -Ph	/	18.66 ± 1.95
10v	t-Butyl	2-Thienyl	/	32.74 ± 3.34
10w	t-Butyl	2-Furanyl	/	42.68 ± 3.45
10x	t-Butyl	Cyclopentyl	/	66.54 ± 4.26
10y	t-Butyl	2-Naphthyl	/	46.87 ± 3.44
11a	t-Butyl	4-F-Ph	n-Butyl	10.46 ± 0.84
11b	t-Butyl	4-F-Ph	t-Butyl	18.46 ± 1.34
11c	t-Butyl	4-F-Ph	cyclohexyl	20.54 ± 1.68
11d	t-Butyl	4-F-Ph	Ph	30.92 ± 2.57
11e	t-Butyl	4-F-Ph	3,4-(OMe) ₂ -Ph	24.45 ± 3.68
11f	t-Butyl	4-F-Ph	4-F-Ph	36.46 ± 2.57
11g	t-Butyl	4-F-Ph	H	9.12 ± 0.76
Foretinib				1.75 ± 0.14

10e ($IC_{50} = 19.45$ nM; $R_1 = n\text{-Propyl}$, $R_2 = \text{Phenyl}$), compound **10f** ($IC_{50} = 30.38$ nM; $R_1 = \text{Cyclohexyl}$, $R_2 = \text{Phenyl}$) and

Compound **10g** ($IC_{50} = 54.42$ nM; $R_1 = \text{Phenyl}$, $R_2 = \text{Phenyl}$). The t-butyl group could bind mainly with the hydrophobic binding pocket in protein. On the basic understanding of the structural of c-Met, the t-butyl group in compound **10h** may possess a larger spaced structure with hydrophobic properties. This tightly structural variation made compound **10h** bind tightly with surrounding residues, which resulted in lower binding free energy. Accordingly, t-butyl derivatives were further studied in the following work.

Comprehensive t-butyl analogs with diverse R_2 substituents, including fourteen aryl rings, an aromatic fused ring, two heterocyclic groups and a cyclopentyl were investigated to further discover the structure-activity relationships. The SARs based on IC_{50} values indicated that the R_2 group played an important role for the c-Met kinase inhibitory efficacy. Indeed, the introduction of mono-EDGs 4-methyl **10i** ($R_2 = 4\text{-Me-Phenyl}$, $IC_{50} = 12.35$ nM) and 4-methoxy **10j** ($R_2 = 4\text{-OMe-Phenyl}$, $IC_{50} = 21.48$ nM) led to a 1.5- and 2.6-fold decrease in potency in comparison with **10h** that no substituent on the phenyl ring ($R_2 = \text{Phenyl}$, $IC_{50} = 8.35$ nM). The introduction of trisubstituted-EDGs **10k** ($R_2 = 3,4,5\text{-(OMe)}_3\text{-Phenyl}$, $IC_{50} = 35.64$ nM) reduced the potency by another 1.7-fold compared to **10j**. The results showed that the presence of electron-donating group decreased the c-Met inhibitory activity of the target compounds. Moreover, the more the number of electron-

donating groups, the lower the activities, such as **10j** and **10k**. In view of these results, the utilization of EDGs was not further pursued. Gratifyingly, the introduction of EWGs exhibited positive effect on the c-Met inhibitory activity. In particular, incorporation of the mono-EWGs at the 4-position of phenyl ring (**10m**, $R_2 = 4\text{-F-Phenyl}$, $IC_{50} = 2.43$ nM, increased 3.4-fold) showed a higher potency than that of mono-EWGs at 3-position and 2-position of the phenyl (**10o**, $R_2 = 3\text{-F-Ph}$, $IC_{50} = 4.72$ nM, increased 1.8-fold; **10p**, $R_2 = 2\text{-F-Ph}$, $IC_{50} = 3.13$ nM, increased 2.7-fold), and the same trend was observed for the series of chloro-substituted phenyl compounds **10p** ($R_2 = 4\text{-Cl-Phenyl}$, $IC_{50} = 7.43$ nM), **10q** ($R_2 = 3\text{-Cl-Phenyl}$, $IC_{50} = 7.86$ nM), and **10r** ($R_2 = 2\text{-Cl-Phenyl}$, $IC_{50} = 8.12$ nM). However, the introduction of double electron-withdrawing groups (**10u**, $R_2 = 3,4\text{-Cl-Phenyl}$, $IC_{50} = 18.66$ nM) showed opposite trend in potency of the compound compared with 4-chloro derivative **10p** and 3-chloro derivative **10q**, which indicated a mono-substituted phenyl ring is more preferred than a disubstituted phenyl ring. The introduction of strong EWGs to the phenyl ring led to a significantly decrease in activities compared with **10h** ($R_2 = \text{Ph}$, $IC_{50} = 8.35$ nM), such as compound **10t** ($R_2 = 4\text{-CF}_3\text{-Ph}$, $IC_{50} = 36.62$ nM) that caused the potency to be lowered by 4.4-fold, suggesting that the phenyl probably need medium electron density. The bulky effect of the substituents likely weakened the potency since the more steric analogs 4-(t-butyl)phenyl **10l** ($IC_{50} = 18.45$ nM, decreased 2.2-fold) and 2-naphthyl **10y** ($IC_{50} = 46.87$ nM, decreased 2.2-fold) and 2-naphthyl **10y** ($IC_{50} = 46.87$ nM, decreased 2.2-fold)

($IC_{50} = 46.87$ nM, decreased 5.6-fold) showed obvious decreased activity compared with **10h** ($R_2 = \text{Phenyl}$). The loss of activity might due to that the hydrophobic pocket of c-Met was probably not sufficiently large to accommodate with the bulky groups.

Compared with **10h** ($R_2 = \text{Phenyl}$), five-membered heterocyclic groups were also explored, such as 2-thienyl derivative **10v** ($IC_{50} = 32.74$ nM) and 2-furanyl analogue **10w** ($IC_{50} = 42.68$ nM), which led to 3.9- to 5.1-fold loss activity against c-Met kinase, suggesting that the electron-rich five membered ring made an adverse effect. More importantly, the replacement of the phenyl ring with cyclopentyl group **10x** ($IC_{50} = 66.54$ nM) resulted in 7.9-fold loss activity, indicating that π -aryl interaction really plays an essential role in the biological activity.

Having identified well tolerated groups on R_1 (*t*-Butyl) and R_2 (4-F-Phenyl), respectively, our attention was turned to focus on the linker in the subsequent efforts, and seven target compounds **11a-g** were prepared. To our delight, α -acylaminoamide derivative **11a** ($R_3 = n\text{-Butyl}$, $IC_{50} = 10.46$ nM) exhibited moderate c-Met kinase inhibitory efficacy. Encouraged by the remarkably potency of compound **11a**, it was continued for further investigation focused on R_3 group. Compared to target compound **11a**, the introduction of diverse substitution patterns on R_3 including *t*-butyl (**11b**, $IC_{50} = 18.46$ nM), cyclohexyl (**11c**, $IC_{50} = 20.54$ nM), phenyl rings (**11d**, $R_3 = \text{Phenyl}$, $IC_{50} = 30.92$ nM; **11e**, $R_3 = 3,4\text{-(OMe)}_2\text{-Phenyl}$, $IC_{50} = 24.45$ nM; **11f**, $R_3 = 4\text{-F-Phenyl}$, $IC_{50} = 36.46$ nM) caused significantly activity decreases. However, with the introduction of H atom on R_3 , compound **11g** ($R_3 = \text{H}$, $IC_{50} = 9.12$ nM, increased 1.1-fold) displayed a slight increase on c-Met inhibitory efficacy in comparison with **11a** ($R_3 = n\text{-Butyl}$, $IC_{50} = 10.46$ nM). The results suggested that electronic effect and steric hindrance of R_3 group were fairly sensitive to the c-Met kinase inhibitory activities. Further studies about the effect of R_3 group (α -acylaminoamide) are in progress in our laboratory and will be reported upon in the future.

Considering the enantiomers of candidate compounds might display different activities, the two enantiomers of the representative compound **10m** were prepared by chiral chromatography, which were used for the investigation of the effect of the enantiomers on c-Met inhibition. Unexpectedly, the two enantiomers displayed similar activity on c-Met inhibition. Thus, racemic **10m** was used for further biological evaluation *in vitro*.

The pharmacological data suggested that a suitable degree of electron density and steric hindrance on the 5-atom linker was essential to improve the c-Met kinase inhibitory activity. Moreover, the data showed that the hydrophobic pocket can accommodate the mono-EWGs of phenyl (moiety B), especially F or Cl at *para*-position of phenyl rings.

2.2. *In vitro* antiproliferative activity

The synthesized thirty-two target compounds (**10a-y**, **11a-g**) were evaluated for their cytotoxicity *in vitro* against c-Met-addicted cancer cell lines, including H460 (human lung cancer), HT-29 (human colon cancer), MKN-45 (human gastric cancer) and a c-Met less sensitive MDA-MB-231 (human breast cancer) by the MTT-based assay, taking foretinib as positive control. The results expressed as half-maximal inhibitory concentration (IC_{50}) values and were presented in Table 3, as mean values of experiments performed in triplicate.

As illustrated in Table 3, most of the target compounds showed moderate-to-excellent cytotoxic activity against different cancer cells, and four of them exhibited more or similar potent activities against certain cancer lines in comparison with foretinib, indicating that the introduction of α -acyloxycarboxamide or α -acylaminoamide moiety as the 5-atom linker maintained remarkably the potent cytotoxicity, and α -acyloxycarboxamide-contained target compounds **10a-y** exhibited higher potency than α -

acylaminoamide-contained target compounds **11a-g**. It was noteworthy that most of the target compounds displayed good anti-proliferative potency against H460 and HT-29, and relatively poor potency toward the other two cell lines, which suggested that these two series of target compounds may possessed selectivity for H460 and HT-29 cancer cell lines. Particularly, the most promising compound **10m** displayed excellent cytotoxicity against H460, HT-29 and MDA-MB-231 cell lines with IC_{50} values of 0.14 ± 0.03 μM , 0.20 ± 0.02 μM and 0.42 ± 0.03 μM , respectively, which were 1.3–1.7 times superior to foretinib (IC_{50} : 0.24 ± 0.04 μM , 0.26 ± 0.03 μM , and 0.65 ± 0.05 μM , respectively). The study of structure-activity relationships (SARs) indicated that these analogs showed similar SARs as summarized in the c-Met kinase level: (a) target compounds bearing α -acyloxycarboxamide generally exhibited higher potency than compounds bearing α -acylaminoamide linkage; (b) the target compounds showed excellent selectivity toward H460 and HT-29 cancer cell lines; (c) the EWGs (such as F, Cl) on moiety B benefited to the potency; (d) introduction of steric hindrance (4-(*t*-Butyl)-Ph and 2-naphthyl) or bulky electron-withdrawing groups to phenyl ring (suchas Br and CF_3) led to an obvious decrease in cytotoxicity; (e) the cytotoxicity of compounds with substituent (mono-EWGs) at 4-positionof phenyl ring (moiety B) was higher than those with substituents at other positions.

2.2.3. Enzymatic selectivity assays

To examine the selectivity of compound **10m** on c-Met kinase over other kinases, it was screened against 6 other tyrosine kinases (Table 4). Compared with its high potency against c-Met ($IC_{50} = 2.43$ nM), **10m** also exhibited high inhibitory effects against c-Kit ($IC_{50} = 4.42$ nM), Flt-3 ($IC_{50} = 6.15$ nM) and Ron ($IC_{50} = 18.64$ nM). **10m** exhibited less inhibitory effects against VEGFR-2 and Flt-4, the potency was 121- and 222-fold lower than against c-Met, respectively. Additionally, **10m** exhibited a slight or no tyrosine kinase inhibitory activity against EGFR ($IC_{50} > 10$ μM). These data suggested that compound **10m** is a promising multi-target inhibitor of tyrosine kinase, and might act through some other mechanism rather than only by inhibiting c-Met kinase. Further studies on the mechanism of these compounds are in progress.

2.2.4. Concentration-dependent assay

In order to investigate the relationship between activity and concentration, seven concentrations of compound **10m** were set and the inhibitory rate of compound **10m** against four cancer cell lines for 72 h was measured by MTT assay, and the results were shown in Fig. 4. It can be seen that the inhibition rate of compound **10m** against four cancer cell lines increased with the increase of concentration. The results showed that the target compound **10m** inhibited the growth of the four tumor cell lines in a concentration-dependent manner.

2.2.5. Time-dependent assay

In order to examine whether the time can affect the inhibitory effect of the compound against tumor cells, five concentrations of compound **10m** and three time gradients were set and the inhibition rate of H460 cell was measured by MTT assay. The results were shown in Fig. 5. At each concentration, the inhibition rate of compound **10m** against H460 cell increased with time. In addition, at the same time, the inhibition rate of compound **10m** against H460 cell increased with increasing concentration. Therefore, compound **10m** can inhibit the proliferation of H460 cell in a time and concentration dependent manner.

Table 3Structures and cytotoxic activities of compounds **10a-y** and **11a-g** against H460, HT-29, MKN-45 and MDA-MB-231 cell lines *in vitro*.

Compd.	R ₁	R ₂	R ₃	IC ₅₀ (μmol/L) ± SD			
				H460	HT-29	MKN-45	MDA-MB-231
10a	Methyl	Cyclopentyl	/	15.19 ± 1.34	24.56 ± 1.40	28.20 ± 2.47	ND
10b	Methyl	2-Thienyl	/	2.46 ± 0.27	4.02 ± 0.33	6.39 ± 0.29	8.24 ± 0.56
10c	Methyl	2-Naphthyl	/	9.43 ± 1.16	11.57 ± 1.34	15.65 ± 1.21	13.26 ± 1.09
10d	Methyl	Ph	/	1.29 ± 0.22	1.92 ± 0.17	2.39 ± 0.19	3.21 ± 0.18
10e	<i>n</i> -Propyl	Ph	/	0.89 ± 0.15	1.24 ± 0.22	1.87 ± 0.25	2.48 ± 0.21
10f	Cyclohexyl	Ph	/	10.32 ± 0.65	15.64 ± 1.13	20.54 ± 1.95	17.95 ± 1.31
10g	Phenyl	Ph	/	22.45 ± 2.56	25.62 ± 1.89	ND	ND
10h	<i>t</i> -Butyl	Ph	/	0.40 ± 0.10	0.45 ± 0.04	0.56 ± 0.06	0.65 ± 0.14
10i	<i>t</i> -Butyl	4-Me-Ph	/	0.78 ± 0.11	0.85 ± 0.13	1.08 ± 0.09	1.42 ± 0.16
10j	<i>t</i> -Butyl	4-OMe-Ph	/	1.25 ± 0.11	1.54 ± 0.17	1.86 ± 0.14	2.58 ± 0.33
10k	<i>t</i> -Butyl	3,4,5-(OMe) ₃ -Ph	/	2.70 ± 0.36	3.03 ± 0.28	3.87 ± 0.15	4.92 ± 0.36
10l	<i>t</i> -Butyl	4-(<i>t</i> -Butyl)-Ph	/	2.06 ± 0.12	2.45 ± 0.34	3.95 ± 0.52	4.45 ± 0.29
10m	<i>t</i> -Butyl	4-F-Ph	/	0.14 ± 0.03	0.20 ± 0.02	0.26 ± 0.04	0.42 ± 0.03
10n	<i>t</i> -Butyl	3-F-Ph	/	0.26 ± 0.04	0.30 ± 0.05	0.54 ± 0.11	0.49 ± 0.06
10o	<i>t</i> -Butyl	2-F-Ph	/	0.21 ± 0.05	0.24 ± 0.03	0.38 ± 0.06	0.44 ± 0.05
10p	<i>t</i> -Butyl	4-Cl-Ph	/	0.20 ± 0.04	0.24 ± 0.03	0.32 ± 0.05	0.48 ± 0.06
10q	<i>t</i> -Butyl	3-Cl-Ph	/	0.31 ± 0.06	0.39 ± 0.05	0.60 ± 0.07	0.86 ± 0.16
10r	<i>t</i> -Butyl	2-Cl-Ph	/	0.22 ± 0.02	0.29 ± 0.04	0.46 ± 0.08	0.76 ± 0.12
10s	<i>t</i> -Butyl	4-Br-Ph	/	0.48 ± 0.12	0.56 ± 0.14	0.75 ± 0.10	0.90 ± 0.14
10t	<i>t</i> -Butyl	4-CF ₃ -Ph	/	1.84 ± 0.26	2.16 ± 0.18	2.87 ± 0.23	3.52 ± 0.34
10u	<i>t</i> -Butyl	3,4-(Cl) ₂ -Ph	/	0.78 ± 0.08	0.90 ± 0.12	1.12 ± 0.21	1.56 ± 0.14
10v	<i>t</i> -Butyl	2-Thienyl	/	0.96 ± 0.13	1.26 ± 0.22	1.70 ± 0.23	1.89 ± 0.38
10w	<i>t</i> -Butyl	2-Furanyl	/	2.68 ± 0.25	2.96 ± 0.30	ND	3.56 ± 0.26
10x	<i>t</i> -Butyl	Cyclopentyl	/	11.56 ± 0.78	9.27 ± 0.65	11.54 ± 1.10	13.98 ± 1.85
10y	<i>t</i> -Butyl	2-Naphthyl	/	3.34 ± 0.36	4.38 ± 0.24	ND	6.75 ± 0.68
11a	<i>t</i> -Butyl	4-F-Ph	<i>n</i> -Butyl	0.47 ± 0.07	0.52 ± 0.05	0.68 ± 0.04	0.86 ± 0.05
11b	<i>t</i> -Butyl	4-F-Ph	<i>t</i> -Butyl	1.30 ± 0.05	1.45 ± 0.09	1.58 ± 0.11	1.70 ± 0.13
11c	<i>t</i> -Butyl	4-F-Ph	cyclohexyl	4.34 ± 0.25	5.35 ± 0.45	6.65 ± 0.52	8.48 ± 0.72
11d	<i>t</i> -Butyl	4-F-Ph	Ph	7.56 ± 0.78	9.27 ± 0.65	11.54 ± 1.10	13.98 ± 1.35
11e	<i>t</i> -Butyl	4-F-Ph	3,4-(OMe) ₂ -Ph	6.42 ± 0.67	6.21 ± 0.78	7.52 ± 0.51	8.87 ± 0.92
11f	<i>t</i> -Butyl	4-F-Ph	4-F-Ph	8.42 ± 0.64	10.23 ± 0.56	12.43 ± 1.62	14.77 ± 1.46
11g	<i>t</i> -Butyl	4-F-Ph	H	0.38 ± 0.06	0.44 ± 0.07	0.65 ± 0.03	0.96 ± 0.14
Foretinib^a				0.24 ± 0.04	0.26 ± 0.03	0.050 ± 0.005	0.65 ± 0.05

Bold values show the IC₅₀ values of the prepared compounds lower than the values of the positive control foretinib. ND: Not determined.^a Used as a positive control.**Table 4**
Kinase selectivity profile of compound **10m** and foretinib.

Enzyme	Enzyme IC ₅₀ (nM)	
	10m	Foretinib
c-kit	4.42	6.74
Flt-3	6.15	5.56
Ron	18.64	3.62
VEGFR-2	295	4.96
Flt-4	540	1.67
EGFR	>10,000	3020
c-Met	2.43	1.75

2.3. Molecular docking studies

To further explore the binding mode of target compounds with the active site of c-Met, molecular docking simulation studies were carried out by using Autodock 4.2 package. Based on the *in vitro* inhibition results, we selected compound **10m**, the best c-Met inhibitor in this study, as ligand example, and the structure of c-Met was selected as the docking model (PDB ID code: 3LQ8). The binding modes of compound **10m** and c-Met was shown in Fig. 6, and the nitrogen atom of quinoline, the oxygen atom of α -acyloxy-carboxamide moiety in compound **10m** formed two H-bond interactions with protein residue Met1160 and Asp1222, respectively. At the same time, one π - π interaction between the phenyl ring and the Phe1223 has been formed. Moreover, the terminal 4-fluorophenyl ring fitted into the hydrophobic pocket that was formed Phe1200, Gln1123, Ile1130 and Phe1124, etc. To gain more structural information for further optimization, docking model of

compound **10m** in the cocrystal structure of foretinib bound to the c-Met kinase were performed simultaneously. It was found that most parts of the compound **10m** overplayed perfectly except for the 3-morpholinopropoxy group in foretinib. The alignment of the two structures showed that they occupy the same area of the protein, and thus result in adonor-acceptor interaction with Met1160 and Asp1222, respectively. In general, these results of the molecular docking study showed that 4-phenoxyquinoline derivatives containing α -acyloxycarboxamide moiety could act synergistically to interact with the binding site of c-Met, suggesting that α -acyloxycarboxamide moiety could serve as a scaffold from which to build a novel series of c-Met inhibitors.

3. Conclusion

In summary, isocyanide-involved multicomponent reactions have been used for the rapid and efficient synthesis of two series of structurally diverse derivatives based on 6,7-disubstituted-4-(2-fluorophenoxy)quinoline. This approach is a valuable tool in design and synthesis of novel c-Met inhibitors with advantages of simplicity, atom-economy, and good yields. The entire target compounds were investigated for their *in vitro* biological activities against c-Met kinase and four cancer cell lines (H460, HT-29, MKN-45 and MDA-MB-231). Most of compounds displayed moderate-to-excellent activity against H460, HT-29 cancer cell lines and relatively poor potent towards MKN-45 and MDA-MB-231 cell lines. In particular, the most promising compound **10m** (c-Met IC₅₀ = 2.43 nM) demonstrated excellent c-Met inhibitory activity and remarkable cytotoxicities against H460, HT-29 and MDA-MB-

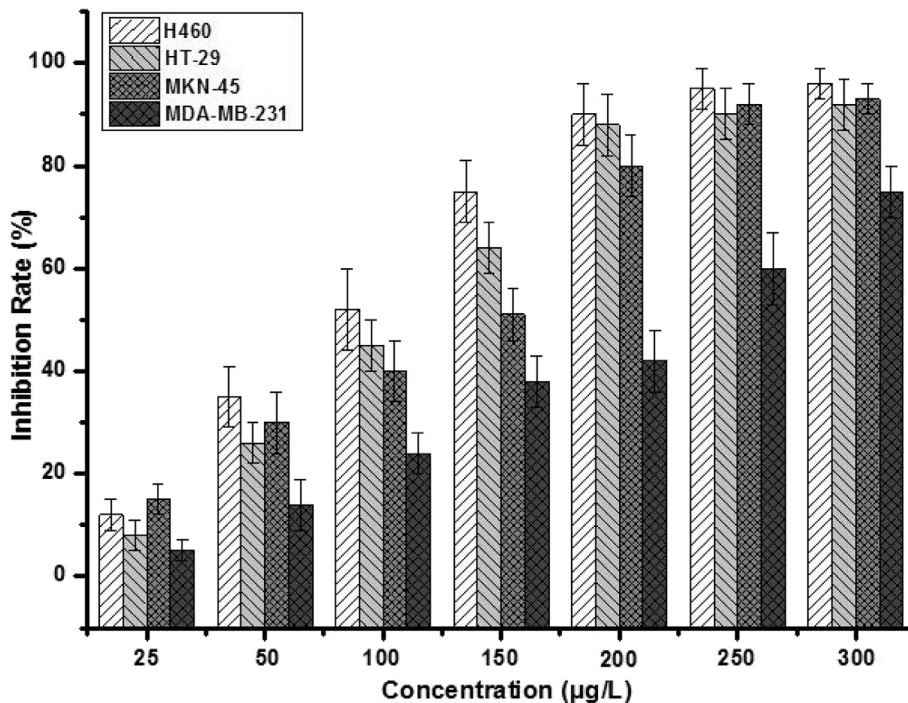


Fig. 4. Relationship between activity and concentration of compound **10m** against four cancer cell lines.

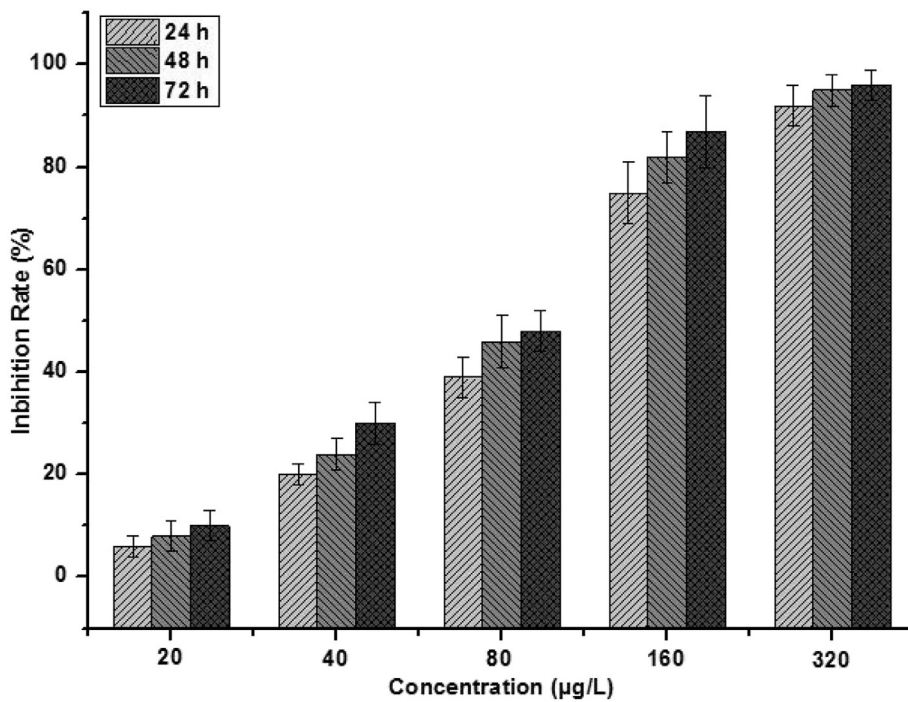


Fig. 5. The inhibitory effect of compound **10m** on H460 cell line at different time points.

231 with IC₅₀ values of 0.14 µM, 0.20 µM, 0.42 µM, which were 1.7-, 1.3- and 1.6-fold superior to positive foretinib, respectively. The preliminary SARs studies indicated that the introduction of α -acyloxycarboxamide or α -acylaminoamide as the 5-atom linker maintained the potent activity, and the potency of α -acyloxycarboxamide analogs was generally more active than that of α -acylaminoamide analogs. The target compounds modified with R₁

and R₃ (R₁ = *t*-butyl, R₃ = H) were favorable to activity, and mono-EWGs (such as 4-F, 4-Cl) on the terminal phenyl rings (moiety B) were also beneficial for improving antitumor activity. Future applications could also involve development of versatile biologically significant 4-phenoxyquinoline fragments into MCR products, chemical libraries created via MCRs, and heterocycles built from isocyanides.

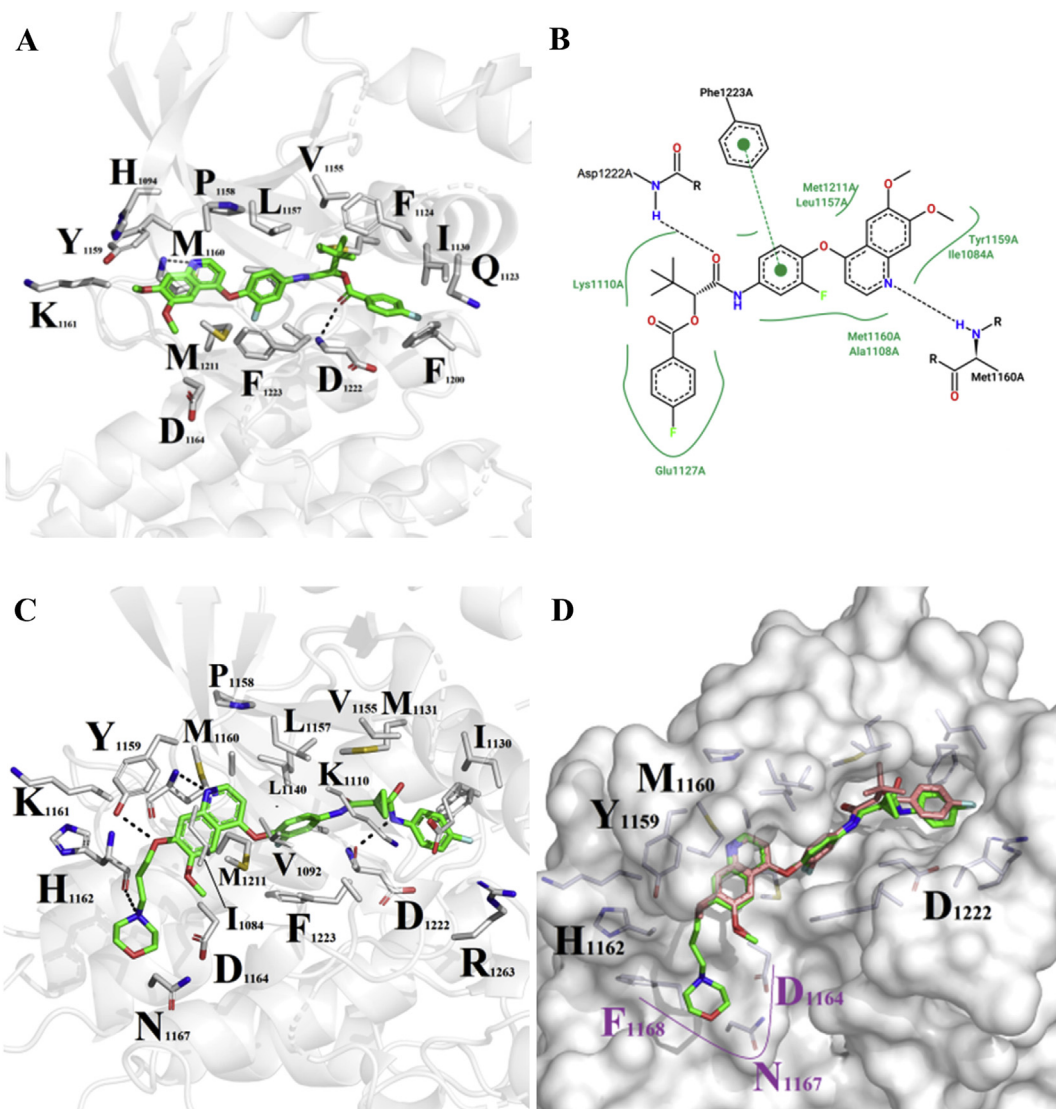


Fig. 6. Binding model comparison of designed compounds with foretinib. (A) Binding pose of compound **10m** with c-Met active site. Compound **10m** was showed in colored sticks, green: carbon atom, blue: nitrogen atom, pink: oxygen atom. (B) The interaction details between compound **10m** and c-Met. (C) Binding pose of foretinib with c-Met active site. (D) Overlay of **10m** (pink color) in the same cavity along with foretinib (green color) as the reference molecule. (For interpretation of the references to color in this figure legend, the reader is referred to the Web version of this article.)

4. Experimental

4.1. Chemistry

Unless otherwise noted, all common reagents and materials were purchased from commercial sources and were used without further purification. Organic solvents were routinely dried and/or distilled prior to use and stored over molecular sieves under argon. Organic extracts were, in general, dried over anhydrous sodium sulfate (Na_2SO_4). TLC plates were visualized by exposure to ultra violet light (UV). Column chromatography was run on silica gel (200–300 mesh) from Qingdao Ocean Chemicals (Qingdao, Shandong, China). Mass spectra were recorded on a Bruker Daltonics APEXII49e spectrometer with ESI source as ionization. Melting points were measured by using a Gongyi X-5 microscopy digital melting point apparatus and are uncorrected. ^1H NMR and ^{13}C NMR spectra were obtained by using a Bruker Advance III 400 MHz NMR spectrometer with TMS as an internal standard. Data are represented as follows: chemical shift, multiplicity (s = singlet,

d = doublet, t = triplet, q = quartet, m = multiplet, br = broad), integration, and coupling constant in Hertz (Hz). Elemental analysis was performed on an Elemental Analyzer vario EL Cube instrument.

4.1.1. General procedure for preparation of 4-((6,7-dimethoxyquinolin-4-yl)oxy)-3-fluoroaniline (7)

The preparation of the key intermediate 4-((6,7-Dimethoxyquinolin-4-yl)oxy)-3-fluoroaniline **7** was achieved in seven steps from commercially available 1-(4-hydroxy-3-methoxyphenyl)ethanone as shown in Scheme 1, which was illustrated in detail in our previous study [69] and thus was not be listed here.

4.1.2. Synthesis of *N*-(3-fluoro-4-(6,7-dimethoxyquinolin-4-yloxy)phenyl)formamide (8)

A round-bottomed flask fitted with a reflux condenser was treated with **7** (1.57 g, 5.0 mmol) and 4.60 g (5.0 mL) of ethyl formate. The mixture was stirred and heated at reflux while 0.55 g (0.75 mL) of triethylamine was added, and afterward for another

18 h. After cooling at room temperature, the reaction mixture was concentrated, followed by addition of water (25 mL). The obtained residue was submitted to extraction with EtOAc (3×50 mL). The organic layer was separated, dried over anhydrous sodium sulfate, filtered, and concentrated. The crude product was purified by silica gel chromatography eluted with ethyl acetate/hexane (2:1) to give compound **8** (1.40 g) as a white solid, yield: 81.8%, m.p.: 201–203 °C. ¹H NMR (400 MHz, DMSO-*d*₆) δ 10.52 (s, 1H), 8.46 (d, *J* = 4.4 Hz, 1H), 8.34 (s, 1H), 8.12 (s, 1H), 7.83 (d, *J* = 12.4 Hz, 1H), 7.51 (s, 1H), 7.42 (m, 2H), 6.44 (d, *J* = 3.6 Hz, 1H), 3.93 (s, 6H). ¹³C NMR (100 MHz, DMSO-*d*₆) δ 163.1, 160.1, 159.3, 153.5 (d, *J* = 244.8 Hz), 152.7, 149.5, 148.9, 146.4, 135.9 (d, *J* = 12.2 Hz), 124.3, 116.0 (d, *J* = 2.6 Hz), 114.5, 108.1 (d, *J* = 22.7 Hz), 107.9, 102.1, 99.0, 55.8 (2C). Anal. Calcd. For C₁₈H₁₅FN₂O₄: C, 63.15; H, 4.42; N, 8.18. Found: C, 63.16; H, 4.44; N, 8.17. ESI-MS: *m/z* 343.1 [M+H]⁺.

4.1.3. Synthesis of 3-fluoro-4-(6,7-dimethoxyquinolin-4-yloxy)phenylisocyanide (**9**)

A solution of **8** (1.36 g, 4.0 mmol) and Et₃N (1.68 mL, 12.0 mmol) in CHCl₃ (12.0 mL) was cooled at 0 °C, then phosphorous oxychloride (0.44 mL, 4.8 mmol) was added dropwise. The reaction was allowed to proceed at 0 °C for 30 min and then at room temperature for an additional 8 h with continuous stirring. After the reaction was completed, an aqueous saturated solution of sodium carbonate was added to quench the reaction at a sufficiently slow rate in order to maintain 10–15 °C. After stirring for 1 h at room temperature, more water (20 mL) and CHCl₃ (20 mL) were added and the organic layer was washed with water (3 × 20 mL), dried with sodium sulfate, and evaporated. The residue was purified by column chromatography (hexane/ethyl acetate = 1:2) to yield the compound **9** (1.20 g) as a pale yellow solid, yield: 92.0%, m.p.: 164–167 °C. ¹H NMR (400 MHz, DMSO-*d*₆) δ 8.49 (d, *J* = 4.8 Hz, 1H), 7.94 (d, *J* = 10.8 Hz, 1H), 7.57–7.54 (m, 2H), 7.47 (s, 1H), 7.41 (s, 1H), 6.57 (d, *J* = 5.2 Hz, 1H), 3.94 (s, 6H). ¹³C NMR (100 MHz, DMSO-*d*₆) δ 165.3, 158.3, 153.4 (d, *J* = 249.0 Hz), 152.8, 149.7, 148.8, 146.6, 142.3 (d, *J* = 11.7 Hz), 124.7, 124.5 (d, *J* = 3.5 Hz), 116.7, 116.4, 114.7, 107.9, 103.1, 98.6, 55.8 (2C). Anal. Calcd. For C₁₈H₁₃FN₂O₃: C, 66.66; H, 4.04; N, 8.64. Found: C, 66.68; H, 4.03; N, 8.66. ESI-MS: *m/z* 325.1 [M+H]⁺.

4.1.4. General procedure for synthesis of 6,7-dimethoxy-4-(2-fluorophenoxy)quinoline derivatives bearing α-acyloxycarboxamide moiety **10a–y**

To a solution of aldehyde/ketone (0.4 mmol) in THF/H₂O (0.5 mL, v/v = 3:1) was added carboxylic acid (0.4 mmol) and **9** (0.2 mmol) at room temperature. The reaction mixture was subsequently heated at 40 °C for 24 h. Upon completion of the reaction (TLC monitoring), the mixture was cooled to room temperature and solvent was evaporated. The residue was purified by chromatography on silica gel using ethyl acetate/hexane as eluent to give **10a–y**.

4.1.4.1. 1-((4-((6,7-Dimethoxyquinolin-4-yl)oxy)-3-fluorophenyl)amino)-1-oxopropan-2-yl cyclopentanecarboxylate (**10a**). White solid, yield: 65.6%, m.p.: 82–85 °C. ¹H NMR (400 MHz, DMSO-*d*₆) δ 10.53 (s, 1H), 8.46 (d, *J* = 5.2 Hz, 1H), 7.84 (dd, *J* = 1.6, 12.8 Hz, 1H), 7.52 (s, 1H), 7.47 (dd, *J* = 2.0, 9.2 Hz, 1H), 7.43 (d, *J* = 8.8 Hz, 1H), 7.40 (s, 1H), 6.45 (d, *J* = 5.2 Hz, 1H), 5.05 (q, *J* = 6.8 Hz, 1H), 3.94 (s, 6H), 2.87–2.79 (m, 1H), 1.86–1.68 (m, 4H), 1.62–1.51 (m, 4H), 1.45 (d, *J* = 6.8 Hz, 3H). ¹³C NMR (100 MHz, DMSO-*d*₆) δ 175.4, 169.4, 159.5, 153.5 (d, *J* = 244.1 Hz), 152.8, 149.6, 148.6, 146.1, 137.7 (d, *J* = 10.0 Hz), 135.7 (d, *J* = 12.4 Hz), 124.2, 116.1 (d, *J* = 2.9 Hz), 114.5, 108.1 (d, *J* = 23.0 Hz), 107.6, 102.1, 99.0, 69.8, 55.8 (2C), 42.6, 29.5, 29.3, 25.5, 25.4, 17.3. Anal. Calcd. For C₂₆H₂₇FN₂O₆: C, 64.72; H, 5.64; N, 5.81. Found: C, 64.74; H, 5.65; N,

5.84. ESI-MS: *m/z* 483.2 [M+H]⁺.

4.1.4.2. 1-((4-((6,7-Dimethoxyquinolin-4-yl)oxy)-3-fluorophenyl)amino)-1-oxopropan-2-yl thiophene-2-carboxylate (**10b**). White solid, yield: 76.8%, m.p.: 105–107 °C. ¹H NMR (400 MHz, DMSO-*d*₆) δ 10.70 (s, 1H), 8.45 (d, *J* = 4.8 Hz, 1H), 7.99 (d, *J* = 4.8 Hz, 1H), 7.88–7.85 (m, 2H), 7.52 (s, 1H), 7.49–7.43 (m, 2H), 7.39 (s, 1H), 7.25–7.24 (m, 1H), 6.44 (d, *J* = 4.8 Hz, 1H), 5.27 (q, *J* = 6.4 Hz, 1H), 3.93 (s, 6H), 1.57 (d, *J* = 6.4 Hz, 3H). ¹³C NMR (100 MHz, DMSO-*d*₆) δ 169.0, 161.0, 159.3, 153.5 (d, *J* = 244.0 Hz), 152.7, 149.5, 148.9, 146.4, 137.7 (d, *J* = 9.8 Hz), 135.8 (d, *J* = 12.3 Hz), 134.5, 134.3, 132.4, 128.5, 124.2, 116.2, 114.5, 108.2 (d, *J* = 23.0 Hz), 107.9, 102.1, 99.0, 70.9, 55.8 (2C). Anal. Calcd. For C₂₅H₂₁FN₂O₆: C, 60.48; H, 4.26; N, 5.64. Found: C, 60.51; H, 4.27; N, 5.66. ESI-MS: *m/z* 497.1 [M+H]⁺.

4.1.4.3. 1-((4-((6,7-Dimethoxyquinolin-4-yl)oxy)-3-fluorophenyl)amino)-1-oxopropan-2-yl 2-naphthoate (**10c**). White solid, yield: 81.6%, m.p.: 122–124 °C. ¹H NMR (400 MHz, DMSO-*d*₆) δ 10.66 (s, 1H), 8.70 (s, 1H), 8.46 (d, *J* = 5.2 Hz, 1H), 8.17 (d, *J* = 8.0 Hz, 1H), 8.08–8.01 (m, 3H), 7.88 (d, *J* = 12.8 Hz, 1H), 7.70–7.61 (m, 2H), 7.52 (s, 1H), 7.49–7.41 (m, 2H), 7.39 (s, 1H), 6.45 (d, *J* = 4.8 Hz, 1H), 5.37 (q, *J* = 6.8 Hz, 1H), 3.93 (s, 6H), 1.66 (d, *J* = 6.4 Hz, 3H). ¹³C NMR (100 MHz, DMSO-*d*₆) δ 169.3, 165.5, 159.4, 153.5 (d, *J* = 244.4 Hz), 152.7, 149.5, 148.8, 146.3, 137.6 (d, *J* = 9.8 Hz), 135.8 (d, *J* = 12.1 Hz), 135.2, 132.1, 130.9, 129.4, 128.8, 128.5, 127.8, 127.1, 126.5, 124.9, 124.2, 116.2, 114.5, 108.2 (d, *J* = 22.9 Hz), 107.8, 102.1, 99.0, 71.0, 55.8 (2C). Anal. Calcd. For C₃₁H₂₅FN₂O₆: C, 68.88; H, 4.66; N, 5.18. Found: C, 68.85; H, 4.67; N, 5.20. ESI-MS: *m/z* 541.2 [M+H]⁺.

4.1.4.4. 1-((4-((6,7-Dimethoxyquinolin-4-yl)oxy)-3-fluorophenyl)amino)-1-oxopropan-2-yl benzoate (**10d**). White solid, yield: 72.4%, m.p.: 91–93 °C. ¹H NMR (400 MHz, DMSO-*d*₆) δ 10.70 (s, 1H), 8.46 (d, *J* = 5.6 Hz, 1H), 8.02 (d, *J* = 7.2 Hz, 2H), 7.87 (dd, *J* = 2.0, 12.8 Hz, 1H), 7.68 (t, *J* = 7.2 Hz, 1H), 7.56 (d, *J* = 7.6 Hz, 2H), 7.53 (s, 1H), 7.50 (dd, *J* = 1.6, 9.2 Hz, 1H), 7.44 (d, *J* = 8.8 Hz, 1H), 7.40 (s, 1H), 6.46 (d, *J* = 4.8 Hz, 1H), 5.31 (q, *J* = 6.8 Hz, 1H), 3.94 (s, 6H), 1.61 (d, *J* = 6.8 Hz, 3H). ¹³C NMR (100 MHz, DMSO-*d*₆) δ 169.2, 165.3, 159.5, 153.5 (d, *J* = 244.2 Hz), 152.8, 149.6, 148.6, 146.1, 137.7 (d, *J* = 9.9 Hz), 135.8 (d, *J* = 12.3 Hz), 133.6, 129.4 (2C), 129.3, 128.8 (2C), 124.2, 116.2 (d, *J* = 2.5 Hz), 114.5, 108.2 (d, *J* = 23.0 Hz), 107.6, 102.1, 99.0, 70.8, 55.8 (2C). Anal. Calcd. For C₂₇H₂₃FN₂O₆: C, 66.12; H, 4.73; N, 5.71. Found: C, 66.13; H, 4.75; N, 5.72. ESI-MS: *m/z* 491.2 [M+H]⁺.

4.1.4.5. 1-((4-((6,7-Dimethoxyquinolin-4-yl)oxy)-3-fluorophenyl)amino)-1-oxopentan-2-yl benzoate (**10e**). White solid, yield: 68.3%, m.p.: 99–101 °C. ¹H NMR (400 MHz, DMSO-*d*₆) δ 10.62 (s, 1H), 8.45 (d, *J* = 4.8 Hz, 1H), 8.03 (d, *J* = 7.6 Hz, 2H), 7.86 (d, *J* = 13.2 Hz, 1H), 7.69 (t, *J* = 7.6 Hz, 1H), 7.58–7.54 (m, 2H), 7.52 (s, 1H), 7.48–7.41 (m, 2H), 7.39 (s, 1H), 6.45 (d, *J* = 5.2 Hz, 1H), 5.19 (t, *J* = 7.2 Hz, 1H), 3.93 (s, 6H), 1.98–1.91 (m, 2H), 1.56–1.49 (m, 2H), 0.97 (t, *J* = 7.2 Hz, 3H). ¹³C NMR (100 MHz, DMSO-*d*₆) δ 168.7, 165.5, 159.4, 153.5 (d, *J* = 244.3 Hz), 152.7, 149.5, 148.9, 146.4, 137.6 (d, *J* = 9.7 Hz), 135.8 (d, *J* = 12.3 Hz), 133.8, 129.5 (2C), 129.2, 128.9 (2C), 124.3, 116.2 (d, *J* = 1.5 Hz), 114.6, 108.2 (d, *J* = 22.6 Hz), 107.9, 102.1, 99.0, 74.2, 55.8 (2C), 33.4, 18.3, 13.7. Anal. Calcd. For C₂₉H₂₇FN₂O₆: C, 67.17; H, 5.25; N, 5.40. Found: C, 67.18; H, 5.27; N, 5.41. ESI-MS: *m/z* 519.2 [M+H]⁺.

4.1.4.6. 1-((4-((6,7-Dimethoxyquinolin-4-yl)oxy)-3-fluorophenyl)carbamoyl)cyclohexyl benzoate (**10f**). White solid, yield: 45.2%, m.p.: 203–205 °C. ¹H NMR (400 MHz, DMSO-*d*₆) δ 10.24 (s, 1H), 8.44 (d, *J* = 4.8 Hz, 1H), 8.06 (d, *J* = 7.6 Hz, 1H), 7.85 (d, *J* = 12.8 Hz, 2H), 7.69 (t, *J* = 6.8 Hz, 1H), 7.59–7.54 (m, 3H), 7.51 (s, 1H), 7.39–7.35 (m, 2H), 6.43 (d, *J* = 4.8 Hz, 1H), 3.93 (s, 6H), 2.34–2.31 (m, 2H), 1.93–1.88 (m, 2H), 1.69–1.57 (m, 4H), 1.35–1.28 (m, 2H). ¹³C NMR (100 MHz, DMSO-*d*₆) δ 171.2, 164.5, 159.4, 153.3 (d, *J* = 244.1 Hz),

152.7, 149.5, 148.8, 146.4, 137.9 (d, $J = 9.4$ Hz), 135.7 (d, $J = 12.1$ Hz), 133.6, 130.0, 129.6 (2C), 128.8 (2C), 123.8, 116.9 (d, $J = 2.3$ Hz), 114.5, 108.9 (d, $J = 22.9$ Hz), 107.8, 102.1, 99.0, 81.7, 55.8 (2C), 31.5 (2C), 24.6, 21.2 (2C). Anal. Calcd. For $C_{31}H_{29}FN_2O_6$: C, 68.37; H, 5.37; N, 5.14. Found: C, 68.38; H, 5.37; N, 5.16. ESI-MS: m/z 545.2 [M+H]⁺.

4.1.4.7. 2-((4-((6,7-Dimethoxyquinolin-4-yl)oxy)-3-fluorophenyl)amino)-2-oxo-1-phenylethyl benzoate (**10g**). White solid, yield: 40.8%, m.p.: 93–95 °C. ¹H NMR (400 MHz, DMSO-d₆) δ 10.96 (s, 1H), 8.42 (d, $J = 3.6$ Hz, 1H), 8.07 (d, $J = 7.2$ Hz, 2H), 7.84 (d, $J = 12.8$ Hz, 1H), 7.73–7.69 (m, 3H), 7.59–7.55 (m, 2H), 7.50–7.41 (m, 6H), 7.39 (s, 1H), 6.44 (d, $J = 4.4$ Hz, 1H), 6.26 (s, 1H), 3.93 (s, 6H). ¹³C NMR (100 MHz, DMSO-d₆) δ 167.1, 165.3, 159.3, 153.5 (d, $J = 244.7$ Hz), 152.7, 149.5, 148.8, 146.3, 137.4 (d, $J = 9.8$ Hz), 135.9 (d, $J = 12.5$ Hz), 134.9, 133.9, 129.5 (2C), 129.1, 129.0 (2C), 128.8 (2C), 128.6, 127.5 (2C), 124.3, 116.1 (d, $J = 2.6$ Hz), 114.5, 108.1 (d, $J = 21.7$ Hz), 107.8, 102.1, 99.0, 75.8, 55.8 (2C). Anal. Calcd. For $C_{32}H_{25}FN_2O_6$: C, 69.56; H, 4.56; N, 5.07. Found: C, 69.57; H, 4.55; N, 5.10. ESI-MS: m/z 553.2 [M+H]⁺.

4.1.4.8. 1-((4-((6,7-Dimethoxyquinolin-4-yl)oxy)-3-fluorophenyl)amino)-3,3-dimethyl-1-oxobutan-2-yl benzoate (**10h**). White solid, yield: 85.6%, m.p.: 129–131 °C. ¹H NMR (400 MHz, DMSO-d₆) δ 10.65 (s, 1H), 8.45 (d, $J = 5.2$ Hz, 1H), 8.04 (d, $J = 8.0$ Hz, 2H), 7.87 (dd, $J = 1.6$, 12.8 Hz, 1H), 7.70 (t, $J = 7.2$ Hz, 1H), 7.57 (t, $J = 7.6$ Hz, 2H), 7.51 (s, 1H), 7.48 (dd, $J = 2.0$, 9.2 Hz, 1H), 7.44 (d, $J = 8.8$ Hz, 1H), 7.39 (s, 1H), 6.46 (d, $J = 5.2$ Hz, 1H), 4.90 (s, 1H), 3.93 (s, 6H), 1.13 (s, 9H). ¹³C NMR (100 MHz, DMSO-d₆) δ 167.3, 165.5, 159.4, 153.5 (d, $J = 244.5$ Hz), 152.7, 149.5, 148.9, 146.4, 137.4 (d, $J = 9.8$ Hz), 135.9 (d, $J = 12.3$ Hz), 133.8, 129.4 (2C), 129.2, 129.0 (2C), 124.3, 116.3 (d, $J = 2.2$ Hz), 114.5, 108.3 (d, $J = 22.9$ Hz), 107.9, 102.2, 99.0, 81.5, 55.8 (2C), 34.0, 26.2 (3C). Anal. Calcd. For $C_{30}H_{29}FN_2O_6$: C, 67.66; H, 5.49; N, 5.26. Found: C, 67.67; H, 5.48; N, 5.27. ESI-MS: m/z 532.2 [M]⁺.

4.1.4.9. 1-((4-((6,7-Dimethoxyquinolin-4-yl)oxy)-3-fluorophenyl)amino)-3,3-dimethyl-1-oxobutan-2-yl 4-methylbenzoate (**10i**). White solid, yield: 81.4%, m.p.: 118–120 °C. ¹H NMR (400 MHz, DMSO-d₆) δ 10.64 (s, 1H), 8.44 (d, $J = 5.6$ Hz, 1H), 7.92 (d, $J = 8.0$ Hz, 2H), 7.87 (dd, $J = 2.0$, 12.8 Hz, 1H), 7.51 (s, 1H), 7.48 (dd, $J = 2.0$, 9.2 Hz, 1H), 7.44 (d, $J = 8.8$ Hz, 1H), 7.39 (s, 1H), 7.36 (d, $J = 8.0$ Hz, 2H), 6.46 (d, $J = 5.2$ Hz, 1H), 4.88 (s, 1H), 3.93 (s, 6H), 2.38 (s, 3H), 1.12 (s, 9H). ¹³C NMR (100 MHz, DMSO-d₆) δ 167.3, 165.5, 159.4, 153.5 (d, $J = 244.2$ Hz), 152.7, 149.5, 148.9, 146.4, 144.2, 137.4 (d, $J = 9.6$ Hz), 135.8 (d, $J = 12.2$ Hz), 129.6 (2C), 129.5 (2C), 126.6, 124.3, 116.3 (d, $J = 1.9$ Hz), 114.6, 108.2 (d, $J = 22.8$ Hz), 107.9, 102.2, 99.0, 80.9, 55.8 (2C), 34.0, 26.2 (3C), 21.3. Anal. Calcd. For $C_{31}H_{31}FN_2O_6$: C, 68.12; H, 5.72; N, 5.13. Found: C, 68.14; H, 5.70; N, 5.15. ESI-MS: m/z 547.2 [M+H]⁺.

4.1.4.10. 1-((4-((6,7-Dimethoxyquinolin-4-yl)oxy)-3-fluorophenyl)amino)-3,3-dimethyl-1-oxobutan-2-yl 4-methoxybenzoate (**10j**). White solid, yield: 82.7%, m.p.: 127–129 °C. ¹H NMR (400 MHz, DMSO-d₆) δ 10.62 (s, 1H), 8.44 (d, $J = 5.2$ Hz, 1H), 7.98 (d, $J = 8.8$ Hz, 2H), 7.87 (d, $J = 13.2$ Hz, 1H), 7.51 (s, 1H), 7.48 (dd, $J = 2.0$, 9.2 Hz, 1H), 7.43 (d, $J = 8.8$ Hz, 1H), 7.39 (s, 1H), 7.08 (d, $J = 8.8$ Hz, 2H), 6.45 (d, $J = 4.8$ Hz, 1H), 4.85 (s, 1H), 3.93 (s, 6H), 3.83 (s, 3H), 1.11 (s, 9H). ¹³C NMR (100 MHz, DMSO-d₆) δ 167.4, 165.2, 163.5, 159.4, 153.5 (d, $J = 244.3$ Hz), 152.7, 149.5, 148.9, 146.4, 137.5 (d, $J = 10.1$ Hz), 135.8 (d, $J = 12.3$ Hz), 131.6 (2C), 124.3, 121.4, 116.3, 114.6, 114.3 (2C), 108.2 (d, $J = 23.1$ Hz), 107.9, 102.2, 99.0, 80.8, 55.8 (2C), 55.7, 34.0, 26.2 (3C). Anal. Calcd. For $C_{31}H_{31}FN_2O_7$: C, 66.18; H, 5.55; N, 4.98. Found: C, 66.20; H, 5.58; N, 4.99. ESI-MS: m/z 563.2 [M+H]⁺.

4.1.4.11. 1-((4-((6,7-Dimethoxyquinolin-4-yl)oxy)-3-fluorophenyl)amino)-3,3-dimethyl-1-oxobutan-2-yl 3,4,5-trimethoxybenzoate

(**10k**). White solid, yield: 78.6%, m.p.: 123–125 °C. ¹H NMR (400 MHz, DMSO-d₆) δ 10.63 (s, 1H), 8.45 (d, $J = 5.2$ Hz, 1H), 7.87 (dd, $J = 1.6$, 12.8 Hz, 1H), 7.51 (s, 1H), 7.47 (dd, $J = 2.0$, 9.2 Hz, 1H), 7.44 (d, $J = 8.8$ Hz, 1H), 7.39 (s, 1H), 7.29 (s, 2H), 6.46 (d, $J = 5.2$ Hz, 1H), 4.86 (s, 1H), 3.93 (s, 6H), 3.84 (s, 6H), 3.74 (s, 3H), 1.13 (s, 9H). ¹³C NMR (100 MHz, DMSO-d₆) δ 167.2, 165.1, 159.4, 153.5 (d, $J = 244.2$ Hz), 152.9 (2C), 152.7, 149.5, 148.9, 146.4, 142.2, 137.4 (d, $J = 9.8$ Hz), 135.9 (d, $J = 12.5$ Hz), 124.3 (d, $J = 4.6$ Hz), 116.3, 114.5, 108.2 (d, $J = 23.2$ Hz), 107.9, 106.6 (2C), 102.2, 99.0, 81.2, 60.3, 56.0 (2C), 55.8 (2C), 34.0, 26.2 (3C). Anal. Calcd. For $C_{33}H_{35}FN_2O_9$: C, 63.66; H, 5.67; N, 4.50. Found: C, 63.68; H, 5.68; N, 4.48. ESI-MS: m/z 623.2 [M+H]⁺.

4.1.4.12. 1-((4-((6,7-Dimethoxyquinolin-4-yl)oxy)-3-fluorophenyl)amino)-3,3-dimethyl-1-oxobutan-2-yl 4-(tert-butyl)benzoate (**10l**). White solid, yield: 75.2%, m.p.: 133–135 °C. ¹H NMR (400 MHz, DMSO-d₆) δ 10.59 (s, 1H), 8.44 (d, $J = 5.2$ Hz, 1H), 7.96 (d, $J = 8.8$ Hz, 2H), 7.87 (dd, $J = 2.0$, 13.2 Hz, 1H), 7.58 (d, $J = 8.4$ Hz, 2H), 7.51 (s, 1H), 7.48 (dd, $J = 2.0$, 8.8 Hz, 1H), 7.44 (d, $J = 8.8$ Hz, 1H), 7.39 (s, 1H), 6.46 (d, $J = 4.8$ Hz, 1H), 4.87 (s, 1H), 3.93 (s, 6H), 1.29 (s, 9H), 1.12 (s, 9H). ¹³C NMR (100 MHz, DMSO-d₆) δ 167.3, 165.5, 159.4, 156.9, 153.5 (d, $J = 244.9$ Hz), 152.7, 149.5, 148.9, 146.4, 137.4 (d, $J = 10.3$ Hz), 135.8 (d, $J = 12.1$ Hz), 129.4 (2C), 126.6, 125.8 (2C), 124.3, 116.3, 114.5, 108.2 (d, $J = 23.1$ Hz), 107.9, 102.2, 99.0, 80.9, 55.8 (2C), 35.0, 34.0, 30.9 (3C), 26.2 (3C). Anal. Calcd. For $C_{34}H_{37}FN_2O_6$: C, 69.37; H, 6.34; N, 4.76. Found: C, 69.39; H, 6.36; N, 4.77. ESI-MS: m/z 589.3 [M+H]⁺.

4.1.4.13. 1-((4-((6,7-Dimethoxyquinolin-4-yl)oxy)-3-fluorophenyl)amino)-3,3-dimethyl-1-oxobutan-2-yl 4-fluorobenzoate (**10m**). White solid, yield: 74.7%, m.p.: 122–124 °C. ¹H NMR (400 MHz, DMSO-d₆) δ 10.72 (s, 1H), 8.44 (d, $J = 5.2$ Hz, 1H), 8.11 (td, $J = 2.0$, 3.2, 3.6 Hz, 2H), 7.88 (dd, $J = 2.4$, 13.2 Hz, 1H), 7.51 (s, 1H), 7.49–7.45 (m, 1H), 7.42 (d, $J = 4.0$ Hz, 1H), 7.40–7.37 (m, 3H), 6.45 (d, $J = 4.8$ Hz, 1H), 4.91 (s, 1H), 3.93 (s, 6H), 1.12 (s, 9H). ¹³C NMR (100 MHz, DMSO-d₆) δ 167.2, 165.5 (d, $J = 250.8$ Hz), 164.6, 159.4, 153.5 (d, $J = 244.3$ Hz), 152.7, 149.5, 148.9, 146.4, 137.4 (d, $J = 9.6$ Hz), 135.8 (d, $J = 12.5$ Hz), 132.4 (d, $J = 9.6$ Hz, 2C), 125.8 (d, $J = 2.1$ Hz), 124.3, 116.3 (2C), 116.1, 114.6, 108.3 (d, $J = 23.1$ Hz), 107.9, 102.2, 99.0, 81.2, 55.8 (2C), 34.0, 26.2 (3C). Anal. Calcd. For $C_{30}H_{28}F_2N_2O_6$: C, 65.45; H, 5.13; N, 5.09. Found: C, 65.43; H, 5.15; N, 5.10. ESI-MS: m/z 551.2 [M+H]⁺.

4.1.4.14. 1-((4-((6,7-Dimethoxyquinolin-4-yl)oxy)-3-fluorophenyl)amino)-3,3-dimethyl-1-oxobutan-2-yl 3-fluorobenzoate (**10n**). White solid, yield: 74.5%, m.p.: 111–113 °C. ¹H NMR (400 MHz, DMSO-d₆) δ 10.57 (s, 1H), 8.46 (d, $J = 5.2$ Hz, 1H), 7.90 (d, $J = 7.6$ Hz, 1H), 7.86 (dd, $J = 2.0$, 12.8 Hz, 1H), 7.75 (d, $J = 8.8$ Hz, 1H), 7.66–7.55 (m, 2H), 7.52 (s, 1H), 7.47 (dd, $J = 2.0$, 9.2 Hz, 1H), 7.44 (d, $J = 8.4$ Hz, 1H), 7.40 (s, 1H), 6.48 (d, $J = 5.2$ Hz, 1H), 4.91 (s, 1H), 3.94 (s, 6H), 1.13 (s, 9H). ¹³C NMR (100 MHz, DMSO-d₆) δ 167.0, 164.4, 162.0 (d, $J = 244.1$ Hz), 159.4, 153.5 (d, $J = 244.4$ Hz), 152.7, 149.5, 148.7, 146.2, 137.2 (d, $J = 9.8$ Hz), 135.9 (d, $J = 12.3$ Hz), 131.4 (d, $J = 7.5$ Hz), 131.3 (d, $J = 7.9$ Hz), 125.6 (d, $J = 2.4$ Hz), 124.2, 120.9 (d, $J = 21.0$ Hz), 116.3 (d, $J = 2.9$ Hz), 115.9 (d, $J = 22.8$ Hz), 114.5, 108.3 (d, $J = 22.9$ Hz), 107.7, 102.2, 99.0, 81.4, 55.8 (2C), 33.9, 26.1 (3C). Anal. Calcd. For $C_{30}H_{28}F_2N_2O_6$: C, 65.45; H, 5.13; N, 5.09. Found: C, 65.46; H, 5.14; N, 5.08. ESI-MS: m/z 573.2 [M+Na]⁺.

4.1.4.15. 1-((4-((6,7-Dimethoxyquinolin-4-yl)oxy)-3-fluorophenyl)amino)-3,3-dimethyl-1-oxobutan-2-yl 2-fluorobenzoate (**10o**). White solid, yield: 62.5%, m.p.: 113–115 °C. ¹H NMR (400 MHz, DMSO-d₆) δ 10.58 (s, 1H), 8.45 (d, $J = 5.2$ Hz, 1H), 7.98 (td, $J = 1.6$, 7.6 Hz, 1H), 7.86 (dd, $J = 2.0$, 12.8 Hz, 1H), 7.75–7.70 (m, 1H), 7.52 (s, 1H), 7.48 (dd, $J = 2.0$, 8.8 Hz, 1H), 7.44 (d, $J = 8.4$ Hz, 1H), 7.41–7.36

(m, 3H), 6.47 (d, J = 5.2 Hz, 1H), 4.90 (s, 1H), 3.94 (s, 6H), 1.12 (s, 9H). ^{13}C NMR (100 MHz, DMSO- d_6) δ 167.0, 163.3, 161.3 (d, J = 256.9 Hz), 159.3, 153.5 (d, J = 244.3 Hz), 152.6, 149.5, 148.8, 146.4, 137.3 (d, J = 9.8 Hz), 153.9 (d, J = 12.3 Hz), 132.0, 124.8 (d, J = 3.5 Hz), 124.2, 117.5 (d, J = 9.6 Hz), 117.4, 117.2, 116.3 (d, J = 2.9 Hz), 114.5, 108.3 (d, J = 22.9 Hz), 107.9, 102.2, 99.0, 81.5, 55.8, 55.7, 33.8, 26.0 (3C). Anal. Calcd. For $\text{C}_{30}\text{H}_{28}\text{F}_2\text{N}_2\text{O}_6$: C, 65.45; H, 5.13; N, 5.09. Found: C, 65.47; H, 5.11; N, 5.11. ESI-MS: m/z 551.2 [M+H]⁺.

4.1.4.16. 1-((4-((6,7-Dimethoxyquinolin-4-yl)oxy)-3-fluorophenyl)amino)-3,3-dimethyl-1-oxobutan-2-yl 4-chlorobenzoate (**10p**). White solid, yield: 70.8%, m.p.: 128–130 °C. ^1H NMR (400 MHz, DMSO- d_6) δ 10.67 (s, 1H), 8.44 (d, J = 5.2 Hz, 1H), 8.03 (d, J = 8.4 Hz, 2H), 7.87 (dd, J = 2.0, 12.8 Hz, 1H), 7.63 (d, J = 8.4 Hz, 2H), 7.51 (s, 1H), 7.49 (dd, J = 2.0, 8.8 Hz, 1H), 7.44 (d, J = 8.8 Hz, 1H), 7.39 (s, 1H), 6.45 (d, J = 4.8 Hz, 1H), 4.91 (s, 1H), 3.93 (s, 6H), 1.12 (s, 9H). ^{13}C NMR (100 MHz, DMSO- d_6) δ 167.1, 164.7, 159.4, 153.5 (d, J = 245.0 Hz), 152.7, 149.5, 148.9, 146.4, 138.8, 137.4 (d, J = 9.8 Hz), 135.9 (d, J = 12.2 Hz), 131.3 (2C), 129.2 (2C), 128.0, 124.3, 116.3 (d, J = 1.3 Hz), 114.6, 108.3 (d, J = 20.6 Hz), 107.9, 102.2, 99.0, 81.3, 55.8 (2C), 34.0, 26.1 (3C). Anal. Calcd. For $\text{C}_{30}\text{H}_{28}\text{ClFN}_2\text{O}_6$: C, 63.55; H, 4.98; N, 4.94. Found: C, 63.56; H, 5.01; N, 4.92. ESI-MS: m/z 567.2 [M+H]⁺.

4.1.4.17. 1-((4-((6,7-Dimethoxyquinolin-4-yl)oxy)-3-fluorophenyl)amino)-3,3-dimethyl-1-oxobutan-2-yl 3-chlorobenzoate (**10q**). White solid, yield: 72.3%, m.p.: 108–110 °C. ^1H NMR (400 MHz, DMSO- d_6) δ 10.55 (s, 1H), 8.45 (d, J = 4.8 Hz, 1H), 8.01–7.98 (m, 2H), 7.88–7.78 (m, 2H), 7.62 (t, J = 8.0 Hz, 1H), 7.51 (s, 1H), 7.47–7.42 (m, 2H), 7.39 (s, 1H), 6.46 (d, J = 4.8 Hz, 1H), 4.90 (s, 1H), 3.93 (s, 6H), 1.13 (s, 9H). ^{13}C NMR (100 MHz, DMSO- d_6) δ 166.9, 164.3, 159.3, 153.5 (d, J = 244.4 Hz), 152.7, 149.5, 148.8, 146.4, 137.2 (d, J = 9.6 Hz), 135.9 (d, J = 12.2 Hz), 133.6, 131.2, 131.0, 128.8, 128.1, 124.2, 116.3 (d, J = 2.6 Hz), 114.5, 108.4 (d, J = 23.0 Hz), 107.9, 102.2, 99.0, 81.5, 55.8 (2C), 33.9, 26.1 (3C). Anal. Calcd. For $\text{C}_{30}\text{H}_{28}\text{ClFN}_2\text{O}_6$: C, 63.55; H, 4.98; N, 4.94. Found: C, 63.54; H, 5.00; N, 4.96. ESI-MS: m/z 567.2 [M+H]⁺.

4.1.4.18. 1-((4-((6,7-Dimethoxyquinolin-4-yl)oxy)-3-fluorophenyl)amino)-3,3-dimethyl-1-oxobutan-2-yl 2-chlorobenzoate (**10r**). White solid, yield: 58.6%, m.p.: 103–105 °C. ^1H NMR (400 MHz, DMSO- d_6) δ 10.59 (s, 1H), 8.45 (d, J = 5.2 Hz, 1H), 7.95 (d, J = 8.0 Hz, 1H), 7.87 (dd, J = 2.0, 12.8 Hz, 1H), 7.65–7.60 (m, 2H), 7.54–7.51 (m, 2H), 7.48 (dd, J = 2.4, 9.2 Hz, 1H), 7.44 (d, J = 8.4 Hz, 1H), 7.40 (s, 1H), 6.47 (d, J = 5.2 Hz, 1H), 4.92 (s, 1H), 3.94 (s, 6H), 1.12 (s, 9H). ^{13}C NMR (100 MHz, DMSO- d_6) δ 166.9, 164.6, 159.3, 153.5 (d, J = 244.6 Hz), 152.6, 149.5, 148.8, 146.4, 137.2 (d, J = 9.9 Hz), 135.9 (d, J = 12.1 Hz), 133.8, 132.4, 131.7, 131.1, 128.9, 127.6, 124.2, 116.2 (d, J = 3.3 Hz), 114.5, 108.2 (d, J = 22.7 Hz), 107.9, 102.1, 98.9, 81.7, 55.7 (2C), 33.8, 26.1 (3C). Anal. Calcd. For $\text{C}_{30}\text{H}_{28}\text{ClFN}_2\text{O}_6$: C, 63.55; H, 4.98; N, 4.94. Found: C, 63.55; H, 5.00; N, 4.92. ESI-MS: m/z 567.2 [M+H]⁺.

4.1.4.19. 1-((4-((6,7-Dimethoxyquinolin-4-yl)oxy)-3-fluorophenyl)amino)-3,3-dimethyl-1-oxobutan-2-yl 4-bromobenzoate (**10s**). White solid, yield: 75.8%, m.p.: 114–116 °C. ^1H NMR (400 MHz, DMSO- d_6) δ 10.57 (s, 1H), 8.45 (d, J = 4.4 Hz, 1H), 7.96 (d, J = 7.6 Hz, 2H), 7.85 (d, J = 12.8 Hz, 1H), 7.78 (d, J = 7.2 Hz, 2H), 7.51 (s, 1H), 7.48–7.42 (m, 2H), 7.39 (s, 1H), 6.46 (d, J = 4.8 Hz, 1H), 4.89 (s, 1H), 3.93 (s, 6H), 1.12 (s, 9H). ^{13}C NMR (100 MHz, DMSO- d_6) δ 167.0, 164.9, 159.3, 153.5 (d, J = 244.4 Hz), 152.6, 149.5, 148.9, 146.4, 137.2 (d, J = 9.8 Hz), 135.9 (d, J = 12.3 Hz), 132.1 (2C), 131.3 (2C), 128.4, 127.9, 124.2, 116.3 (d, J = 2.6 Hz), 114.5, 108.3 (d, J = 22.8 Hz), 107.9, 102.2, 99.0, 81.3, 55.8 (2C), 34.0, 26.1 (3C). Anal. Calcd. For $\text{C}_{30}\text{H}_{28}\text{BrFN}_2\text{O}_6$: C, 58.93; H, 4.62; N, 4.58. Found: C, 58.91; H, 4.63; N, 4.59. ESI-MS: m/z 611.1 [M+H]⁺.

4.1.4.20. 1-((4-((6,7-Dimethoxyquinolin-4-yl)oxy)-3-fluorophenyl)amino)-3,3-dimethyl-1-oxobutan-2-yl 4-(trifluoromethyl)benzoate (**10t**). White solid, yield: 74.8%, m.p.: 129–131 °C. ^1H NMR (400 MHz, DMSO- d_6) δ 10.69 (s, 1H), 8.45 (d, J = 5.2 Hz, 1H), 8.23 (d, J = 8.0 Hz, 2H), 7.95 (d, J = 8.0 Hz, 2H), 7.87 (dd, J = 2.0, 13.2 Hz, 1H), 7.51 (s, 1H), 7.48 (dd, J = 2.0, 9.2 Hz, 1H), 7.44 (d, J = 8.8 Hz, 1H), 7.39 (s, 1H), 6.46 (d, J = 5.2 Hz, 1H), 4.95 (s, 1H), 3.93 (s, 6H), 1.14 (s, 9H). ^{13}C NMR (100 MHz, DMSO- d_6) δ 166.9, 164.5, 159.3, 153.5 (d, J = 244.4 Hz), 152.7, 149.5, 148.9, 146.4, 137.3 (d, J = 9.9 Hz), 136.0 (d, J = 12.2 Hz), 133.2 (q, J = 31.8 Hz), 132.9, 130.3 (2C), 126.0 (q, J = 3.2 Hz, 2C), 124.2, 123.8 (q, J = 271.4 Hz), 116.3 (d, J = 2.2 Hz), 114.6, 108.3 (d, J = 22.8 Hz), 107.9, 102.2, 99.0, 81.5, 55.6 (2C), 34.0, 26.1 (3C). Anal. Calcd. For $\text{C}_{31}\text{H}_{28}\text{F}_4\text{N}_2\text{O}_6$: C, 62.00; H, 4.70; N, 4.66. Found: C, 62.02; H, 4.68; N, 4.67. ESI-MS: m/z 601.2 [M+H]⁺.

4.1.4.21. 1-((4-((6,7-Dimethoxyquinolin-4-yl)oxy)-3-fluorophenyl)amino)-3,3-dimethyl-1-oxobutan-2-yl 3,4-dichlorobenzoate (**10u**). White solid, yield: 74.9%, m.p.: 119–121 °C. ^1H NMR (400 MHz, DMSO- d_6) δ 10.56 (s, 1H), 8.45 (d, J = 4.0 Hz, 1H), 8.14 (s, 1H), 7.99 (d, J = 8.0 Hz, 1H), 7.86–7.83 (m, 2H), 7.51 (s, 1H), 7.45 (t, J = 9.2 Hz, 2H), 7.39 (s, 1H), 6.46 (d, J = 4.4 Hz, 1H), 4.91 (s, 1H), 3.93 (s, 6H), 1.13 (s, 9H). ^{13}C NMR (100 MHz, DMSO- d_6) δ 166.8, 163.7, 159.3, 153.5 (d, J = 244.1 Hz), 152.7, 149.5, 148.8, 146.4, 137.2 (d, J = 9.9 Hz), 136.8, 136.0 (d, J = 12.3 Hz), 131.9, 131.4, 130.9, 129.6, 129.4, 124.2, 116.4 (d, J = 1.9 Hz), 114.5, 108.4 (d, J = 22.9 Hz), 107.8, 102.2, 99.0, 81.6, 55.8 (2C), 33.9, 26.1 (3C). Anal. Calcd. For $\text{C}_{30}\text{H}_{27}\text{Cl}_2\text{FN}_2\text{O}_6$: C, 59.91; H, 4.52; N, 4.66. Found: C, 59.90; H, 4.54; N, 4.67. ESI-MS: m/z 601.2 [M+H]⁺.

4.1.4.22. 1-((4-((6,7-Dimethoxyquinolin-4-yl)oxy)-3-fluorophenyl)amino)-3,3-dimethyl-1-oxobutan-2-yl thiophene-2-carboxylate (**10v**). Pale yellow solid, yield: 82.6%, m.p.: 124–126 °C. ^1H NMR (400 MHz, DMSO- d_6) δ 10.65 (s, 1H), 8.44 (d, J = 5.2 Hz, 1H), 8.01 (dd, J = 1.2, 5.2 Hz, 1H), 7.90–7.85 (m, 2H), 7.51 (s, 1H), 7.47 (dd, J = 2.0, 9.2 Hz, 1H), 7.44 (d, J = 8.4 Hz, 1H), 7.39 (s, 1H), 7.26–7.24 (m, 1H), 6.46 (d, J = 5.2 Hz, 1H), 4.85 (s, 1H), 3.93 (s, 6H), 1.10 (s, 9H). ^{13}C NMR (100 MHz, DMSO- d_6) δ 167.0, 161.3, 159.4, 153.5 (d, J = 244.5 Hz), 152.7, 149.5, 148.9, 146.4, 137.4 (d, J = 9.8 Hz), 135.9 (d, J = 12.3 Hz), 134.7, 134.4, 132.2, 128.7, 124.3, 116.3, 114.6, 108.3 (d, J = 23.1 Hz), 107.9, 102.2, 99.0, 81.1, 55.8 (2C), 34.0, 26.1 (3C). Anal. Calcd. For $\text{C}_{28}\text{H}_{27}\text{FN}_2\text{O}_6\text{S}$: C, 62.44; H, 5.05; N, 5.20. Found: C, 62.45; H, 5.07; N, 5.18. ESI-MS: m/z 539.2 [M+H]⁺.

4.1.4.23. 1-((4-((6,7-Dimethoxyquinolin-4-yl)oxy)-3-fluorophenyl)amino)-3,3-dimethyl-1-oxobutan-2-yl furan-2-carboxylate (**10w**). White solid, yield: 79.8%, m.p.: 105–107 °C. ^1H NMR (400 MHz, DMSO- d_6) δ 10.54 (s, 1H), 8.45 (d, J = 5.2 Hz, 1H), 8.03 (d, J = 0.8 Hz, 1H), 7.85 (dd, J = 2.0, 12.8 Hz, 1H), 7.52 (s, 1H), 7.47 (dd, J = 2.4, 9.2 Hz, 1H), 7.44–7.42 (m, 2H), 7.39 (s, 1H), 6.74 (dd, J = 1.6, 3.6 Hz, 1H), 6.47 (d, J = 4.8 Hz, 1H), 4.85 (s, 1H), 3.94 (s, 6H), 1.09 (s, 9H). ^{13}C NMR (100 MHz, DMSO- d_6) δ 166.9, 159.3, 157.6, 153.5 (d, J = 244.4 Hz), 152.7, 149.5, 148.8, 148.2, 146.4, 143.3, 132.2 (d, J = 9.5 Hz), 135.9 (d, J = 12.3 Hz), 124.2, 119.3, 116.3 (d, J = 2.8 Hz), 114.5, 112.5, 108.3 (d, J = 22.8 Hz), 107.9, 102.2, 99.0, 80.8, 55.8 (2C), 33.9, 26.0 (3C). Anal. Calcd. For $\text{C}_{28}\text{H}_{27}\text{FN}_2\text{O}_7$: C, 64.36; H, 5.21; N, 5.36. Found: C, 64.37; H, 5.20; N, 5.36. ESI-MS: m/z 523.2 [M+H]⁺.

4.1.4.24. 1-((4-((6,7-Dimethoxyquinolin-4-yl)oxy)-3-fluorophenyl)amino)-3,3-dimethyl-1-oxobutan-2-yl cyclopentanecarboxylate (**10x**). White solid, yield: 50.7%, m.p.: 106–108 °C. ^1H NMR (400 MHz, DMSO- d_6) δ 10.48 (s, 1H), 8.44 (d, J = 5.2 Hz, 1H), 7.86 (d, J = 13.2 Hz, 1H), 7.51 (s, 1H), 7.47–7.41 (m, 2H), 7.39 (s, 1H), 6.45 (d, J = 5.2 Hz, 1H), 4.65 (s, 1H), 3.93 (s, 6H), 2.90–2.82 (m, 1H), 1.87–1.72 (m, 4H), 1.59–1.54 (m, 4H), 1.02 (s, 9H). ^{13}C NMR (100 MHz, DMSO- d_6) δ 175.5, 167.4, 159.4, 153.5 (d, J = 244.4 Hz),

152.7, 149.5, 148.9, 146.4, 137.4 (d, $J = 10.0$ Hz), 135.8 (d, $J = 12.3$ Hz), 124.3, 116.2 (d, $J = 1.7$ Hz), 114.5, 108.2 (d, $J = 22.9$ Hz), 107.9, 102.1, 99.0, 80.2, 55.8 (2C), 42.9, 33.7, 29.5, 29.2, 26.0 (3C), 25.5, 25.4. Anal. Calcd. For $C_{29}H_{33}FN_2O_6$: C, 66.40; H, 6.34; N, 5.34. Found: C, 66.38; H, 6.35; N, 5.33. ESI-MS: m/z 525.2 [M+H]⁺.

4.1.4.25. 1-((4-((6,7-Dimethoxyquinolin-4-yl)oxy)-3-fluorophenyl)amino)-3,3-dimethyl-1-oxobutan-2-yl 2-naphthoate (**10y**). White solid, yield: 84.6%, m.p.: 134–136 °C. ¹H NMR (400 MHz, DMSO- d_6) δ 10.71 (s, 1H), 8.70 (s, 1H), 8.45 (d, $J = 5.2$ Hz, 1H), 8.18 (d, $J = 8.0$ Hz, 1H), 8.09–8.01 (m, 3H), 7.90 (dd, $J = 2.4, 13.2$ Hz, 1H), 7.70–7.61 (m, 2H), 7.52–7.50 (m, 2H), 7.44 (t, $J = 8.8$ Hz, 1H), 7.39 (s, 1H), 6.46 (d, $J = 5.2$ Hz, 1H), 4.98 (s, 1H), 3.93 (s, 6H), 1.18 (s, 9H). ¹³C NMR (100 MHz, DMSO- d_6) δ 167.3, 165.7, 159.4, 153.5 (d, $J = 244.5$ Hz), 152.7, 149.5, 148.9, 146.4, 137.4 (d, $J = 9.6$ Hz), 135.9 (d, $J = 12.3$ Hz), 135.3, 132.1, 131.0, 129.6, 128.9, 128.7, 127.8, 127.2, 126.5, 124.9, 124.3, 116.3 (d, $J = 2.5$ Hz), 114.6, 108.3 (d, $J = 22.5$ Hz), 107.9, 102.2, 99.0, 81.3, 55.8 (2C), 34.1, 26.3 (3C). Anal. Calcd. For $C_{34}H_{31}FN_2O_6$: C, 70.09; H, 5.36; N, 4.81. Found: C, 70.07; H, 5.38; N, 4.83. ESI-MS: m/z 583.2 [M+H]⁺.

4.1.5. General procedure for synthesis of 6,7-dimethoxy-4-(2-fluorophenoxy)quinoline derivatives bearing α -acylaminoamide moiety **11a-g**

Pivaldehyde (0.4 mmol), carboxylic acid (0.4 mmol), and **9** (0.2 mmol) were added sequentially to a solution of amine (0.4 mmol) in MeOH (1.0 mL) at room temperature. The reaction mixture was heated at 60 °C for 24 h. Upon completion of the reaction (TLC monitoring), the mixture cooled to room temperature and solvent was evaporated. The crude reaction mixture was purified by column chromatography (ethyl acetate/hexane) to give the target products **11a-g**.

4.1.5.1. *N*-Butyl-*N*-(1-((4-((6,7-dimethoxyquinolin-4-yl)oxy)-3-fluorophenyl)amino)-3,3-dimethyl-1-oxobutan-2-yl)-4-fluorobenzamide (**11a**). White solid, yield: 67.3%, m.p.: 97–99 °C. ¹H NMR (400 MHz, DMSO- d_6) δ 10.76 (s, 1H), 8.46 (d, $J = 4.8$ Hz, 1H), 7.87 (d, $J = 12.8$ Hz, 1H), 7.51 (m, 4H), 7.44 (d, $J = 9.2$ Hz, 1H), 7.40 (s, 1H), 7.28 (t, $J = 8.0$ Hz, 2H), 6.45 (d, $J = 4.8$ Hz, 1H), 5.27 (s, 1H), 3.93 (s, 6H), 3.49 (m, 2H), 1.26–0.95 (m, 13H), 0.51 (t, 3H). ¹³C NMR (100 MHz, DMSO- d_6) δ 171.4, 168.2, 162.3 (d, $J = 245.0$ Hz), 159.3, 153.4 (d, $J = 244.3$ Hz), 152.7, 149.5, 148.9, 146.4, 135.9 (d, $J = 11.5$ Hz), 133.8 (d, $J = 3.2$ Hz), 132.1 (d, $J = 9.2$ Hz), 129.1 (d, $J = 7.6$ Hz, 2C), 124.1, 116.6, 115.5 (d, $J = 21.4$ Hz, 2C), 114.6, 108.5 (d, $J = 25.2$ Hz), 107.9, 102.1, 99.0, 69.8, 55.8 (2C), 46.1, 36.9, 32.2, 27.2 (3C), 19.3, 13.1. Anal. Calcd. For $C_{34}H_{37}F_2N_3O_5$: C, 67.42; H, 6.16; N, 6.94. Found: C, 67.40; H, 6.15; N, 6.95. ESI-MS: m/z 606.3 [M+H]⁺.

4.1.5.2. *N*-(tert-Butyl)-*N*-(1-((4-((6,7-dimethoxyquinolin-4-yl)oxy)-3-fluorophenyl)amino)-3,3-dimethyl-1-oxobutan-2-yl)-4-fluorobenzamide (**11b**). White solid, yield: 70.6%, m.p.: 90–92 °C. ¹H NMR (400 MHz, CDCl₃) δ 11.77 (s, 1H), 8.50 (d, $J = 4.8$ Hz, 1H), 7.83 (d, $J = 11.2$ Hz, 1H), 7.61 (m, 3H), 7.47 (s, 1H), 7.35 (d, $J = 8.0$ Hz, 1H), 7.28–7.22 (m, 1H), 7.14 (t, $J = 7.2$ Hz, 2H), 6.46 (d, $J = 4.4$ Hz, 1H), 4.08 (s, 3H), 4.06 (s, 3H), 3.98 (s, 1H), 1.31 (s, 9H), 1.29 (s, 9H). ¹³C NMR (100 MHz, CDCl₃) δ 176.5, 172.2, 164.3 (d, $J = 250.9$ Hz), 160.3, 154.5 (d, $J = 247.8$ Hz), 152.9, 149.6, 148.6, 146.6, 137.4 (d, $J = 9.6$ Hz), 136.8 (d, $J = 12.4$ Hz), 136.2 (d, $J = 3.2$ Hz), 130.3 (2C), 123.7, 116.3 (d, $J = 2.9$ Hz), 115.5 (2C), 109.5 (d, $J = 22.6$ Hz), 107.6, 102.2, 99.5, 75.4, 60.7, 56.1 (2C), 37.0, 31.1 (3C), 30.1 (3C). Anal. Calcd. For $C_{34}H_{37}F_2N_3O_5$: C, 67.42; H, 6.16; N, 6.94. Found: C, 67.43; H, 6.14; N, 6.95. ESI-MS: m/z 606.3 [M+H]⁺.

4.1.5.3. *N*-Cyclohexyl-*N*-(1-((4-((6,7-dimethoxyquinolin-4-yl)oxy)-3-fluorophenyl)amino)-3,3-dimethyl-1-oxobutan-2-yl)-4-

fluorobenzamide (**11c**). White solid, yield: 61.2%, m.p.: 108–110 °C. ¹H NMR (400 MHz, CDCl₃) δ 11.31 (s, 1H), 8.49 (d, $J = 4.0$ Hz, 1H), 7.81 (d, $J = 11.6$ Hz, 1H), 7.60 (s, 1H), 7.53 (m, 2H), 7.45 (s, 1H), 7.31–7.22 (m, 2H), 7.16 (t, $J = 8.0$ Hz, 2H), 6.44 (d, $J = 4.0$ Hz, 1H), 4.07 (s, 3H), 4.05 (s, 3H), 3.82 (s, 1H), 3.64–3.57 (m, 1H), 1.96–1.65 (m, 6H), 1.30 (s, 9H), 1.25–1.07 (m, 4H). ¹³C NMR (100 MHz, CDCl₃) δ 174.6, 171.0, 163.9 (d, $J = 250.0$ Hz), 160.1, 154.3 (d, $J = 247.8$ Hz), 152.8, 149.4, 148.5, 146.5, 137.0 (d, $J = 9.5$ Hz), 136.7 (d, $J = 12.5$ Hz), 132.5, 128.8 (d, $J = 8.5$ Hz, 2C), 123.6, 116.1 (d, $J = 3.0$ Hz), 115.9 (d, $J = 21.8$ Hz, 2C), 115.4, 109.4 (d, $J = 22.6$ Hz), 107.5, 102.1, 99.3, 72.4, 62.9, 56.0 (2C), 36.0, 31.7, 30.8, 29.6 (3C), 25.6, 25.2, 24.5. Anal. Calcd. For $C_{36}H_{39}F_2N_3O_5$: C, 68.45; H, 6.22; N, 6.65. Found: C, 68.46; H, 6.20; N, 6.68. ESI-MS: m/z 632.3 [M+H]⁺.

4.1.5.4. *N*-(1-((4-((6,7-Dimethoxyquinolin-4-yl)oxy)-3-fluorophenyl)amino)-3,3-dimethyl-1-oxobutan-2-yl)-4-fluoro-*N*-Phenylbenzamide (**11d**). White solid, yield: 48.5%, m.p.: 84–86 °C. ¹H NMR (400 MHz, CDCl₃) δ 9.79 (s, 1H), 8.52 (d, $J = 4.0$ Hz, 1H), 7.87 (d, $J = 11.6$ Hz, 1H), 7.61 (s, 1H), 7.48 (s, 1H), 7.33–7.24 (m, 8H), 6.87 (t, $J = 8.0$ Hz, 3H), 6.47 (d, $J = 4.4$ Hz, 1H), 5.00 (s, 1H), 4.09 (s, 3H), 4.07 (s, 3H), 1.22 (s, 9H). ¹³C NMR (100 MHz, CDCl₃) δ 172.6, 169.0, 163.2 (d, $J = 250.1$ Hz), 160.2, 154.4 (d, $J = 248.2$ Hz), 152.9, 149.6, 148.5, 146.5, 137.1 (d, $J = 12.4$ Hz), 136.8 (d, $J = 9.6$ Hz), 131.8 (d, $J = 3.3$ Hz), 130.6 (d, $J = 8.6$ Hz, 2C), 129.2 (2C), 128.8, 127.9 (2C), 123.7, 116.2 (d, $J = 3.0$ Hz), 115.5, 115.0 (d, $J = 21.8$ Hz, 2C), 109.5 (d, $J = 22.8$ Hz), 107.5, 102.2, 99.4, 65.5, 56.1 (2C), 35.7, 28.6 (3C). Anal. Calcd. For $C_{36}H_{33}F_2N_3O_5$: C, 69.11; H, 5.32; N, 6.72. Found: C, 67.13; H, 5.34; N, 6.73. ESI-MS: m/z 626.2 [M+H]⁺.

4.1.5.5. *N*-(3,4-Dimethoxyphenyl)-*N*-(1-((4-((6,7-dimethoxyquinolin-4-yl)oxy)-3-fluorophenyl)amino)-3,3-dimethyl-1-oxobutan-2-yl)-4-fluorobenzamide (**11e**). Pale red solid, yield: 65.4%, m.p.: 102–104 °C. ¹H NMR (400 MHz, DMSO- d_6) δ 10.69 (s, 1H), 8.47 (d, $J = 5.2$ Hz, 1H), 7.89 (d, $J = 13.2$ Hz, 1H), 7.58 (d, $J = 8.8$ Hz, 1H), 7.52 (s, 1H), 7.44 (d, $J = 8.8$ Hz, 1H), 7.40 (s, 1H), 7.32–7.29 (m, 3H), 7.01 (t, $J = 8.8$ Hz, 2H), 6.70–6.66 (m, 2H), 6.43 (d, $J = 5.2$ Hz, 1H), 5.47 (s, 1H), 3.94 (s, 6H), 3.64 (s, 3H), 3.55 (s, 3H), 1.04 (s, 9H). ¹³C NMR (100 MHz, DMSO- d_6) δ 170.9, 168.5, 161.8 (d, $J = 245.0$ Hz), 159.4, 153.4 (d, $J = 244.2$ Hz), 152.7, 149.5, 148.9, 147.8, 147.7, 146.5, 137.9 (d, $J = 9.7$ Hz), 135.8 (d, $J = 12.3$ Hz), 133.8 (d, $J = 2.2$ Hz), 133.6, 132.1 (d, $J = 9.5$ Hz), 130.2 (d, $J = 8.5$ Hz, 2C), 124.1, 116.7, 115.6 (d, $J = 21.6$ Hz), 114.6 (d, $J = 14.9$ Hz, 2C), 114.5, 110.4, 108.7 (d, $J = 22.5$ Hz), 107.9, 102.1, 99.0, 69.8, 65.7, 55.8 (2C), 55.4, 35.6, 27.9 (3C). Anal. Calcd. For $C_{38}H_{37}F_2N_3O_7$: C, 66.56; H, 5.44; N, 6.13. Found: C, 66.55; H, 5.46; N, 6.13. ESI-MS: m/z 686.3 [M+H]⁺.

4.1.5.6. *N*-(1-((4-((6,7-Dimethoxyquinolin-4-yl)oxy)-3-fluorophenyl)amino)-3,3-dimethyl-1-oxobutan-2-yl)-4-fluoro-*N*-(4-fluorophenyl)benzamide (**11f**). White solid, yield: 47.4%, m.p.: 201–203 °C. ¹H NMR (400 MHz, CDCl₃) δ 9.67 (s, 1H), 8.52 (d, 1H), 7.82 (d, $J = 11.6$ Hz, 1H), 7.60 (s, 1H), 7.49 (s, 1H), 7.30 (t, $J = 8.0$ Hz, 1H), 7.21 (m, 5H), 6.94–6.86 (m, 4H), 6.44 (d, $J = 3.6$ Hz, 1H), 5.16 (s, 1H), 4.07 (s, 3H), 4.06 (s, 3H), 1.16 (s, 9H). ¹³C NMR (100 MHz, CDCl₃) δ 172.5, 168.8, 163.0 (d, $J = 250.3$ Hz), 161.5 (d, $J = 250.2$ Hz), 160.2, 154.3 (d, $J = 248.2$ Hz), 153.0, 149.6, 148.4, 146.5, 138.2, 137.1 (d, $J = 12.4$ Hz), 136.6 (d, $J = 9.4$ Hz), 131.6 (d, $J = 3.4$ Hz), 130.9 (d, $J = 6.1$ Hz, 2C), 130.4 (d, $J = 8.5$ Hz, 2C), 123.7, 116.2, 116.1 (d, $J = 25.7$ Hz, 2C), 115.5, 115.1 (d, $J = 21.8$ Hz, 2C), 109.5 (d, $J = 22.9$ Hz), 107.4, 102.1, 99.4, 60.3, 56.1 (2C), 35.5, 28.3 (3C). Anal. Calcd. For $C_{36}H_{32}F_3N_3O_5$: C, 67.18; H, 5.01; N, 6.53. Found: C, 67.16; H, 5.02; N, 6.55. ESI-MS: m/z 644.2 [M+H]⁺.

4.1.5.7. *N*-(1-((4-((6,7-dimethoxyquinolin-4-yl)oxy)-3-fluorophenyl)amino)-3,3-dimethyl-1-oxobutan-2-yl)-4-fluorobenzamide (**11g**). Pale yellow solid, yield: 28.6%, m.p.: 123–125 °C. ¹H NMR

(400 MHz, CDCl₃) δ 11.23 (br s, 1H), 8.41 (d, *J* = 4.0 Hz, 1H), 8.09 (br s, 1H), 7.73 (d, *J* = 11.6 Hz, 1H), 7.52 (s, 1H), 7.45 (t, *J* = 6.0 Hz, 2H), 7.37 (s, 1H), 7.23–7.14 (m, 2H), 7.10–7.06 (m, 2H), 6.36 (d, *J* = 4.0 Hz, 1H), 3.99 (s, 3H), 3.97 (s, 3H), 3.74 (s, 1H), 1.22 (s, 9H). ¹³C NMR (100 MHz, CDCl₃) δ 174.8, 171.2, 164.1 (d, *J* = 250.0 Hz), 160.3, 154.5 (d, *J* = 247.8 Hz), 153.0, 149.6, 148.7, 146.7, 137.2 (d, *J* = 9.5 Hz), 136.9 (d, *J* = 12.5 Hz), 132.7, 129.0 (d, *J* = 8.5 Hz, 2C), 123.8, 116.3 (d, *J* = 3.0 Hz), 116.1 (d, *J* = 21.8 Hz, 2C), 115.6, 109.6 (d, *J* = 22.6 Hz), 107.7, 102.3, 99.5, 70.6, 56.2 (2C), 31.9, 29.8 (3C). Anal. Calcd. For C₃₀H₂₉F₂N₃O₅: C, 65.56; H, 5.32; N, 7.65. Found: C, 65.57; H, 5.34; N, 7.65. ESI-MS: *m/z* 550.3 [M+H]⁺.

4.2. Biology

4.2.1. Cytotoxicity against tumor cells assay

The cancer cells were cultured in minimum essential medium (MEM) supplemented with 10% fetal bovine serum (FBS) [70–72]. Approximately 4 × 10³ cells per well, suspended in MEM medium, were plated onto each well of a 96-well plate and incubated in 5% CO₂ at 37 °C for 24 h. The test compounds were added to the culture medium at the indicated final concentrations and the cell cultures were continued for 72 h. Fresh MTT was added to each well at a final concentration of 5 µg/mL and incubated with cells at 37 °C for 4 h. The formazan crystals were dissolved in 100 µL DMSO per each well, and the absorbency at 492 nm (for the absorbance of MTT formazan) and 630 nm (for the reference wavelength) was measured with the ELISA reader. All compounds were tested three times in each of the cell lines. The results expressed as IC₅₀ (inhibitory concentration of 50%) were the average of three determinations calculated by using the Bacus Laboratories Incorporated Slide Scanner (Bliss) software.

4.2.2. Tyrosine kinases assay

The tyrosine kinases activities were evaluated using homogeneous time-resolved fluorescence (HTRF) assays, as previously reported protocol [73,74]. Briefly, 20 mg/mL poly (Glu, Tyr) 4:1 (Sigma) was preloaded as a substrate in 384-well plates. Then 50 µL of 10 mM ATP (Invitrogen) solution diluted in kinase reaction buffer (50 mM HEPES, pH 7.0, 1 M DTT, 1 M MgCl₂, 1 M MnCl₂, and 0.1% NaN₃) was added to each well. Various concentrations of compounds diluted in 10 µL of 1% DMSO (v/v) were used as the negative control. The kinase reaction was initiated by the addition of purified tyrosine kinase proteins diluted in 39 µL of kinase reaction buffer solution. The incubation time for the reactions was 30 min at 25 °C, and the reactions were stopped by the addition of 5 µL of Streptavidin-XL665 and 5 µL Tk Antibody Cryptate working solution to all of wells. The plates were read using Envision (PerkinElmer) at 320 nm and 615 nm. The inhibition rate (%) was calculated using the following equation: % inhibition 100 = [(Activity of enzyme with tested compounds - Min)/(Max - Min)] × 100 (Max: the observed enzyme activity measured in the presence of enzyme, substrates, and cofactors; Min: the observed enzyme activity in the presence of substrates, cofactors and in the absence of enzyme). IC₅₀ values were calculated from the inhibition curves.

4.3. Docking studies

For docking purposes, the three-dimensional structure of the c-Met (PDB code: 3LQ8) were obtained from RCSB Protein Data Bank [75]. Hydrogen atoms were added to the structure allowing for appropriate ionization at physiological pH. The protonated state of several important residues, such as CYS919, and ASP1046 were adjusted by using SYBYL 6.9.1 (Tripos, St. Louis, USA) in favor of forming reasonable hydrogen bond with the ligand. Molecular

docking analysis was carried out by the Autodock 4.2 package to explore the binding model for the active site of c-Met with its ligand. All atoms located within the range of 5.0 Å from any atom of the cofactor were selected into the active site, and the corresponding amino acid residue was, therefore, involved into the active site if only one of its atoms was selected. Other parameters were all set as default in the docking calculations. All calculations were performed on Silicon Graphics workstation.

Author contributions

X. Nan, S.B. Fang, H.J. Li and Q.Y. Li conducted the research, analyzed the data, and wrote the manuscript. H.J. Li, S.B. Fang and Y.C. Wu designed the study, analyzed the data, wrote the manuscript and commented on the manuscript.

Declaration of competing interest

The authors declare no competing financial interest or personal relationships that could have appeared to influence the work reported in this paper.

Acknowledgements

This work was supported by the Key Research and Development Program of Shandong Province (2019GSF108089), the Natural Science Foundation of Shandong Province (ZR2019MB009), the National Natural Science Foundation of China (21672046, 21372054), and the Found from the Huancui District of Weihai City.

Appendix A. Supplementary data

Supplementary data to this article can be found online at <https://doi.org/10.1016/j.ejmech.2020.112241>.

References

- [1] D.P. Bottaro, J.S. Rubin, D.L. Falletto, A.M.-L. Chan, T.E. Kmiecik, G.F. Vande Woude, S.A. Aaronson, Identification of the hepatocyte growth factor receptor as the c-met proto-oncogene product, *Science* 251 (1991) 802–804.
- [2] M. Dean, M. Park, M.M. Le Beau, T.S. Robins, M.O. Diaz, J.D. Rowley, D.G. Blair, G.F. Vande Woude, The human met oncogene is related to the tyrosine kinase oncogenes, *Nature* 318 (1985) 385–388.
- [3] L. Trusolino, P.M. Comoglio, Scatter-factor and semaphorin receptors: cell signaling for invasive growth, *Nat. Rev. Canc.* 2 (2002) 289–300.
- [4] C. Birchmeier, W. Birchmeier, E. Gherardi, G.F. Vande Woude, Met, metastasis, motility and more, *Nat. Rev. Mol. Cell Biol.* 4 (2003) 915–925.
- [5] W. Gao, J.K. Han, Overexpression of ING5 inhibits HGF-induced proliferation, invasion and EMT in thyroid cancer cells via regulation of the c-Met/PI3K/Akt signaling pathway, *Biomed. Pharmacother.* 98 (2018) 265–270.
- [6] J.A. Aguirre Ghiso, D.F. Alonso, E.F. Farías, D.E. Gomez, E.B. de Kier Joffé, Dereglulation of the signaling pathways controlling urokinase production, *Eur. J. Biochem.* 263 (1999) 295–304.
- [7] S. Rong, S. Segal, M. Anver, J.H. Resau, G.F. Vande Woude, Invasiveness and metastasis of NIH 3T3 cells induced by Met-hepatocyte growth factor/scatter factor autocrine stimulation, *Proc. Natl. Acad. Sci. U.S.A.* 91 (1994) 4731–4735.
- [8] M. Jeffers, S. Rong, M. Anver, G.F. Vande Woude, Autocrine hepatocyte growth factor/scatter factor-Met signaling induces transformation and the invasive/metastatic phenotype in C127 cells, *Oncogene* 13 (1996) 853–856.
- [9] H. Takayama, W.J. LaRochelle, R. Sharp, T. Otsuka, P. Kriebel, M. Anver, S.A. Aaronson, G. Merlini, Diverse tumorigenesis associated with aberrant development in mice overexpressing hepatocyte growth factor/scatter factor, *Proc. Natl. Acad. Sci. U.S.A.* 94 (1997) 701–706.
- [10] T. Otsuka, H. Takayama, R. Sharp, G. Celli, W.J. LaRochelle, D.P. Bottaro, N. Ellmore, W. Vieira, J.W. Owens, M. Anver, G. Merlini, c-Met autocrine activation induces development of malignant melanoma and acquisition of the metastatic phenotype, *Canc. Res.* 58 (1998) 5157–5167.
- [11] S. Baldaccia, Z. Kherrouche, V. Cockenpot, L. Stovena, M.C. Copinb, E. Werkmeister, N. Marchandc, M. Kyheng, D. Tulasnec, A.B. Cortot, MET amplification increases the metastatic spread of EGFR-mutated NSCLC, *Lung Canc.* 125 (2018) 57–67.
- [12] G. Tsakonas, J. Botling, P. Micke, C. Rivardc, L. LaFleur, J. Mattsson, T. Boyle, F.R. Hirsch, S. Ekman, c-MET as a biomarker in patients with surgically

- resected non-small cell lung cancer, *Lung Canc.* 133 (2019) 69–74.
- [13] Y. Toiyama, C. Miki, Y. Inoue, Y. Okugawa, K. Tanaka, M. Kusunoki, Serum hepatocyte growth factor as a prognostic marker for stage II or III colorectal cancer patients, *Int. J. Canc.* 125 (2009) 1657–1662.
- [14] Y.D. Liao, R. Grobholz, U. Abel, L. Trojan, M.S. Michel, P. Angel, D. Mayer, Increase of AKT/PKB expression correlates with gleason pattern in human prostate cancer, *Int. J. Canc.* 107 (2003) 676–680.
- [15] J.G. Christensen, J. Burrows, R. Salgia, c-Met as a target for human cancer and characterization of inhibitors for therapeutic intervention, *Canc. Lett.* 225 (2005) 1–26.
- [16] F. Cappuzzo, A. Marchetti, M. Skokan, E. Rossi, S. Gajapathy, L. Felicioni, M. del Grammstro, M.G. Sciarrotta, F. Buttitta, M. Incarbone, L. Toschi, G. Finocchiaro, A. Destro, L. Terracciano, M. Roncalli, M. Alloisio, A. Santoro, M. Varella-Garcia, Increased MET gene copy number negatively affects survival of surgically resected non-small-cell lung cancer patients, *J. Clin. Oncol.* 27 (2009) 1667–1674.
- [17] J.R. Graff, B.W. Konicek, A.M. McNulty, Z.J. Wang, K. Houck, S. Allen, J.D. Paul, A. Hbaili, R.G. Goode, G.E. Sandusky, R.L. Vessella, B.L. Neubauer, Increased AKT activity contributes to prostate cancer progression by dramatically accelerating prostate tumor growth and diminishing p27^{Kip1} expression, *J. Biol. Chem.* 275 (2000) 24500–24505.
- [18] T. Burgess, A. Coxon, S. Meyer, J. Sun, K. Rex, T. Tsuruda, Q. Chen, S.Y. Ho, L. Li, S. Kaufman, K. McDorman, R.C. Cattley, J. Sun, G. Elliott, K. Zhang, X. Feng, X.C. Jia, L. Green, R. Radinsky, R. Kendall, Fully human monoclonal antibodies to hepatocyte growth factor with therapeutic potential against hepatocyte growth factor/c-Met-dependent human tumors, *Canc. Res.* 66 (2006) 1721–1729.
- [19] H.K. Jin, R.H. Yang, Z. Zheng, M. Romero, J. Ross, H. Bou-Reslan, R.A.D. Carano, I. Kasman, E. Mai, J. Young, J.P. Zha, Z.M. Zhang, S. Ross, R. Schwall, G. Colbern, M. Merchant, MetMAB, the one-armed 5D5 anti-c-Met antibody, inhibits orthotopic pancreatic tumor growth and improves survival, *Canc. Res.* 68 (2008) 4360–4368.
- [20] E.H. van der Horst, L. Chinn, M. Wang, T. Velilla, H. Tran, Y. Madrona, A. Lam, M. Ji, T.C. Hoey, A.K. Sato, Discovery of fully human anti-MET monoclonal antibodies with antitumor activity against colon cancer tumor models *in vivo*, *Neoplasia* 11 (2009) 355–364.
- [21] I. Dussault, S.F. Bellon, From concept to reality: the long road to c-Met and RON receptor tyrosine kinase inhibitors for the treatment of cancer, *Anti Canc. Agents Med. Chem.* 9 (2009) 221–229.
- [22] S.F. Bellon, P. Kaplan-Lefko, Y.J. Yang, Y.H. Zhang, J. Moriguchi, K. Rex, C.W. Johnson, P.E. Rose, A.M. Long, A.B. O'Connor, Y. Gu, A. Coxon, T. Kim, A. Tasker, T.L. Burgess, I. Dussault, c-Met inhibitors with novel binding mode show activity against several hereditary papillary renal cell carcinoma-related mutations, *J. Biol. Chem.* 283 (2008) 2675–2683.
- [23] X. Zhai, G.L. Bao, L.M. Wang, M.K. Cheng, M. Zhao, S.J. Zhao, H.Y. Zhou, P. Gong, Design, synthesis and biological evaluation of novel 4-phenoxy-6,7-disubstituted quinolines possessing (thio) semicarbazones as c-Met kinase inhibitors, *Bioorg. Med. Chem.* 24 (2016) 1331–1345.
- [24] Y.F. Yang, Y. Zhang, Y.L. Yang, LL. Zhao, L.H. Si, H.B. Zhang, Q.S. Liu, J.P. Zhou, Discovery of imidazopyridine derivatives as novel c-Met kinase inhibitors: synthesis, SAR study, and biological activity, *Bioorg. Chem.* 70 (2017) 126–132.
- [25] M.H. El-Wakil, H.M. Ashour, M.N. Saudi, A.M. Hassan, I.M. Labouta, Design, synthesis and molecular modeling studies of new series of antitumor 1,2,4-triazines with potential c-Met kinase inhibitory activity, *Bioorg. Chem.* 76 (2018) 154–165.
- [26] F. Zhao, L.D. Zhang, Y. Hao, N. Chen, R. Bai, Y.J. Wang, C.C. Zhang, G.S. Li, L.J. Hao, C. Shi, J. Zhang, Y. Mao, Y. Fan, G.X. Xia, J.X. Yu, Y.J. Liu, Identification of 3-substituted-6-(1-(1H-[1,2,3]triazolo[4,5-b]pyrazin-1-yl)ethyl)quinoline derivatives as highly potent and selective mesenchymal-epithelial transition factor (c-Met) inhibitors via metabolite profiling-based structural optimization, *Eur. J. Med. Chem.* 134 (2017) 147–158.
- [27] H.L. Yuan, Q.F. Liu, L. Zhang, S.H. Hu, T.T. Chen, H.F. Li, Y.D. Chen, Y.C. Xu, T. Lu, Discovery, optimization and biological evaluation for novel c-Met kinase inhibitors, *Eur. J. Med. Chem.* 143 (2018) 491–502.
- [28] L.S. Zhuo, H.C. Xu, M.S. Wang, X.E. Zhao, Z.H. Ming, X.L. Zhu, W. Huang, G.F. Yang, 2,7-naphthyridinone-based MET kinase inhibitors: a promising novel scaffold for antitumor drug development, *Eur. J. Med. Chem.* 178 (2019) 705–714.
- [29] A.A. Boezio, K.W. Copeland, K. Rex, B.K. Albrecht, D. Bauer, S.F. Bellon, C. Boezio, M.A. Broome, D. Choquette, A. Coxon, I. Dussault, S. Hirai, R. Lewis, M.J. Lin, J. Lohman, J.Z. Liu, E.A. Peterson, M. Potashman, R. Shimanovich, Y. Teffera, D.A. Whittington, K.R. Vaida, J. Harmange, Discovery of (R)-6-(1-(8-fluoro-6-(1-methyl-1H-pyrazol-4-yl)-[1,2,4]triazolo[4,3-a]pyridin-3-yl)ethyl)-3-(2-methoxyethoxy)-1,6-naphthyridin-5(6H)-one (AMG 337), a Potent and Selective Inhibitor of MET with high unbound target coverage and robust *in vivo* antitumor activity, *J. Med. Chem.* 59 (2016) 2328–2342.
- [30] I. Dussault, S.F. Bellon, c-Met inhibitors with different binding modes: two is better than one, *Cell Cycle* 7 (2008) 1157–1160.
- [31] S. Berthou, D.M. Aebersold, L.S. Schmidt, D. Stroka, C. Heigl, B. Streit, D. Stalder, G. Gruber, C.X. Liang, A.R. Howlett, D. Candinas, R.H. Greiner, K.E. Lipson, Y. Zimmer, The Met kinase inhibitor SU11274 exhibits a selective inhibition pattern toward different receptor mutated variants, *Oncogene* 23 (2004) 5387–5393.
- [32] S. Matsumoto, N. Miyamoto, T. Hirayama, H. Oki, K. Okada, M. Tawada, H. Iwata, K. Nakamura, S. Yamasaki, H. Miki, A. Hori, S. Imamura, Structure-based design, synthesis, and evaluation of imidazo[1,2-b]pyridazine and imidazo[1,2-a]pyridine derivatives as novel dual c-Met and VEGFR2 kinase inhibitors, *Bioorg. Med. Chem.* 21 (2013) 7686–7698.
- [33] B.H. Qi, Y. Yang, G.W. Gong, H. He, X.P. Yue, X. Xu, Y. Hu, J.M. Li, T. Chen, X.B. Wan, A.M. Zhang, G.B. Zhou, Discovery of N¹-(4-((7-(3-(4-ethylpiperazin-1-yl)propoxy)-6-methoxyquinolin-4-yl)oxy)-3,5-difluorophenyl)-N²-(2-(2,6-difluorophenyl)-4-oxothiazolidin-3-yl)urea as a multi-tyrosine kinase inhibitor for drug-sensitive and drug-resistant cancers treatment, *Eur. J. Med. Chem.* 163 (2019) 10–27.
- [34] J.J. Cui, M. Tran-Dubé, H. Shen, M. Nambu, P.P. Kung, M. Pairish, L. Jia, J. Meng, L. Funk, I. Botrous, M. McTigue, N. Grodsky, K. Ryan, E. Padrique, G. Alton, S. Timofeevskii, S. Yamazaki, Q.H. Li, H. Zou, J. Christensen, B. Mroczkowski, S. Bender, R.S. Kania, M.P. Edwards, Structure based drug design of crizotinib (PF-02341066), a potent and selective dual inhibitor of mesenchymal-epithelial transition factor (c-MET) kinase and anaplastic lymphoma kinase (ALK), *J. Med. Chem.* 54 (2011) 6342–6363.
- [35] M.M. Liu, Y.L. Hou, W.L. Yin, S.G. Zhou, P. Qian, Z. Guo, L.Y. Xu, Y.F. Zhao, Discovery of a novel 6,7-disubstituted-4-(2-fluorophenoxy)quinolines bearing 1,2,3-triazole-4-carboxamide moiety as potent c-Met kinase inhibitors, *Eur. J. Med. Chem.* 119 (2016) 96–108.
- [36] T.L. Underiner, T. Herbertz, S.J. Miknyoczki, Discovery of small molecule c-Met inhibitors: evolution and profiles of clinical candidates, *Anti Canc. Agents Med. Chem.* 10 (2010) 7–27.
- [37] J. Liu, M.H. Nie, Y.J. Wang, J.X. Hu, F. Zhang, Y.L. Gao, Y.J. Liu, P. Gong, Design, synthesis and structure-activity relationships of novel 4-phenoxyquinoline derivatives containing 1,2,4-triazolone moiety as c-Met kinase inhibitors, *Eur. J. Med. Chem.* 123 (2016) 431–446.
- [38] B.K. Albrecht, J.C. Harmange, D. Bauer, L. Berry, C. Bode, A.A. Boezio, A. Chen, D. Choquette, I. Dussault, C. Fridrich, S. Hirai, D. Hoffman, J.F. Larrow, P. Kaplan-Lefko, J. Lin, J. Lohman, A.M. Long, J. Moriguchi, A. O'Connor, M.H. Potashman, M. Reese, K. Rex, A. Siegmund, K. Shah, R. Shimanovich, S.K. Springer, Y. Teffera, Y.J. Yang, Y.H. Zhang, S.F. Bellon, Discovery and optimization of triazolopyridazines as potent and selective inhibitors of the c-Met kinase, *J. Med. Chem.* 51 (2008) 2879–2882.
- [39] N.D. D'Angelo, S.F. Bellon, S.K. Booker, Y. Chen, A. Coxon, C. Dominguez, I. Fellows, D. Hoffman, R. Hungate, P. Kaplan-Lefko, M.R. Lee, C. Li, B.B. Liu, E. Rainbeau, P.J. Reider, K. Rex, A. Siegmund, Y.X. Sun, A.S. Tasker, N. Xi, S.M. Xu, Y.J. Yang, Y.H. Zhang, T.L. Burgess, I. Dussault, T.S. Kim, Design, synthesis, and biological evaluation of potent c-Met inhibitors, *J. Med. Chem.* 51 (2008) 5766–5779.
- [40] S.J. Zhao, Y. Zhang, H.Y. Zhou, S.C. Xi, B. Zou, G.L. Bao, L.M. Wang, J. Wang, T.F. Zeng, P. Gong, X. Zhai, Synthesis and biological evaluation of 4-(2-fluorophenoxy)-3,3'-bipyridine derivatives as potential c-met inhibitors, *Eur. J. Med. Chem.* 120 (2016) 37–50.
- [41] L.X. Wang, S. Xu, X.B. Liu, X.Y. Chen, H.H. Xiong, S.S. Hou, W.S. Zou, Q.D. Tang, P.W. Zheng, W.F. Zhu, Discovery of thionopyrimidine-triazole conjugates as c-Met targeting and apoptosis inducing agents, *Bioorg. Chem.* 77 (2018) 370–380.
- [42] X.Q. Wang, N. Jiang, S.J. Zhao, S.C. Xi, J. Wang, T.F. Jing, W.Y. Zhang, M. Guo, P. Gong, X. Zhai, Design, synthesis and biological evaluation of novel 4-(2-fluorophenoxy)quinoline derivatives as selective c-Met inhibitors, *Bioorg. Med. Chem.* 25 (2017) 886–896.
- [43] S. Li, Y.F. Zhao, K.W. Wang, Y.L. Gao, J.M. Han, B.B. Cui, P. Gong, Discovery of novel 4-(2-fluorophenoxy)quinoline derivatives bearing 4-oxo-1,4-dihydrocinnoline-3-carboxamide moiety as c-Met kinase inhibitors, *Bioorg. Med. Chem.* 21 (2013) 2843–2855.
- [44] B.H. Qi, Y. Yang, H. He, X.P. Yue, Y.T. Zhou, X. Zhou, Y.Y. Chen, M. Liu, A.M. Zhang, F.C. Wei, Identification of novel N¹-(2-aryl-1,3-thiazolidin-4-one)-N²-aryl ureas showing potent multi-tyrosine kinase inhibitory activities, *Eur. J. Med. Chem.* 146 (2018) 368–380.
- [45] Q.D. Tang, Y.L. Duan, H.H. Xiong, T. Chen, Z. Xiao, L.X. Wang, Y.Y. Xiao, S.M. Huang, Y.H. Xiong, W.F. Zhu, P. Gong, P.W. Zheng, Synthesis and anti-proliferative activity of 6,7-disubstituted-4-phenoxyquinoline derivatives bearing the 1,8-naphthyridin-2-one moiety, *Eur. J. Med. Chem.* 158 (2018) 201–213.
- [46] W.K. Liao, G. Hu, Z. Guo, D.Y. Sun, L.X. Zhang, Y.X. Bu, Y.X. Li, Y.J. Liu, P. Gong, Design and biological evaluation of novel 4-(2-fluorophenoxy)quinoline derivatives bearing an imidazolone moiety as c-Met kinase inhibitors, *Bioorg. Med. Chem.* 23 (2015) 4410–4422.
- [47] J. Liu, D. Yang, X.X. Yang, M.H. Nie, G.D. Wu, Z.C. Wang, W. Li, Y.J. Liu, P. Gong, Design, synthesis and biological evaluation of novel 4-phenoxyquinoline derivatives containing 3-oxo-3,4-dihydroquinoxaline moiety as c-Met kinase inhibitors, *Bioorg. Med. Chem.* 25 (2017) 4475–4486.
- [48] R.W. Armstrong, A.P. Combs, P.A. Tempest, S.D. Brown, T.A. Keating, Multiple-component condensation strategies for combinatorial library synthesis, *Acc. Chem. Res.* 29 (1996) 123–131.
- [49] A. Dömling, Recent developments in isocyanide based multicomponent reactions in applied chemistry, *Chem. Rev.* 106 (2006) 17–89.
- [50] K.C. Nicolaou, D.J. Edmonds, P.G. Bulger, Cascade reactions in total synthesis, *Angew. Chem. Int. Ed.* 45 (2006) 7134–7186.
- [51] D. Enders, C. Grondal, M.R.M. Hüttl, Asymmetric organocatalytic domino reactions, *Angew. Chem. Int. Ed.* 46 (2007) 1570–1581.
- [52] B.B. Touré, D.G. Hall, Natural product synthesis using multicomponent reaction strategies, *Chem. Rev.* 109 (2009) 4439–4486.

- [53] A. Dömling, W. Wang, K. Wang, Chemistry and biology of multicomponent reactions, *Chem. Rev.* 112 (2012) 3083–3135.
- [54] I. Akritopoulou-Zanze, Isocyanide-based multicomponent reactions in drug discovery, *Curr. Opin. Chem. Biol.* 12 (2008) 324–331.
- [55] L. Weber, The application of multi-component reactions in drug discovery, *Curr. Med. Chem.* 9 (2002) 2085–2093.
- [56] C. Hulme, V. Gore, Multi-component reactions: emerging chemistry in drug discovery 'from xylocain to crixivan', *Curr. Med. Chem.* 10 (2003) 51–80.
- [57] A. Dömling, I. Ugi, Multicomponent reactions with isocyanides, *Angew. Chem. Int. Ed.* 39 (2000) 3168–3210.
- [58] A. Dömling, Recent advances in isocyanide-based multicomponent chemistry, *Curr. Opin. Chem. Biol.* 6 (2002) 306–313.
- [59] V. Nair, C. Rajesh, A.U. Vinod, S. Bindu, A.R. Sreekanth, J.S. Mathen, L. Balagopal, Strategies for heterocyclic construction via novel multicomponent reactions based on isocyanides and nucleophilic carbenes, *Acc. Chem. Res.* 36 (2003) 899–907.
- [60] J. Zhang, S.X. Lin, D.J. Cheng, X.Y. Liu, B. Tan, Phosphoric acid-catalyzed asymmetric classic Passerini reaction, *J. Am. Chem. Soc.* 137 (2015) 14039–14042.
- [61] X.H. Zeng, H.M. Wang, M.W. Ding, Unexpected synthesis of 5,6-dihydropyridin-2(1H)-ones by a domino Ugi/Aldol/Hydrolysis reaction starting from Baylis-Hillman phosphonium salts, *Org. Lett.* 17 (2015) 2234–2237.
- [62] I. Ugi, B. Werner, A. Dömling, The chemistry of isocyanides, their multicomponent reactions and their libraries, *Molecules* 8 (2003) 53–66.
- [63] M. Main, J.S. Snaith, M.M. Meloni, M. Jauregui, D. Sykes, S. Faulkner, A.M. Kenwright, Using the Ugi multicomponent condensation reaction to prepare families of chromophore appended azamacrocycles and their complexes, *Chem. Commun.* (2008) 5212–5214.
- [64] S.G. Zhou, H.M. Liao, C. He, Y.N. Dou, M.Y. Jiang, L.X. Ren, Y.F. Zhao, P. Gong, Design, synthesis and structure–activity relationships of novel 4-phenoxyquinoline derivatives containing pyridazinone moiety as potential antitumor agents, *Eur. J. Med. Chem.* 83 (2014) 581–593.
- [65] L.M. Miller, S.C. Mayer, D.M. Berger, D.H. Boschelli, F. Boschelli, L. Di, X.M. Du, M. Dutia, M.B. Floyd, M. Johnson, C. Hess Kenny, G. Krishnamurthy, F. Moy, S. Petusky, D. Tkach, N. Torres, B.Q. Wu, W.X. Xu, Lead identification to generate 3-cyanoquinoline inhibitors of insulin-like growth factor receptor (IGF-1R) for potential use in cancer treatment, *Bioorg. Med. Chem. Lett.* 19 (2009) 62–66.
- [66] L.B. Liu, M.H. Norman, M. Lee, N. Xi, A. Siegmund, A.A. Boezio, S. Booker, D. Choquette, N.D. D'Angelo, J. Germain, K. Yang, Y.J. Yang, Y.H. Zhang, S.F. Bellon, D.A. Whittington, J.C. Harmange, C. Dominguez, T.S. Kim, I. Dussault, Structure-based design of novel class II c-Met inhibitors: 2. SAR and kinase selectivity profiles of the pyrazolone series, *J. Med. Chem.* 55 (2012) 1868–1897.
- [67] V. Estévez, M. Villacampa, J.C. Menéndez, Recent advances in the synthesis of pyrroles by multicomponent reactions, *Chem. Soc. Rev.* 43 (2014) 4633–4657.
- [68] L. Kou, M.J. Wang, L.T. Yan, X.B. Zhao, X. Nan, L. Yang, Y.Q. Liu, S.L. Morris-Natschke, K.H. Lee, Toward synthesis of third-generation spin-labeled podophyllotoxin derivatives using isocyanide multicomponent reactions, *Eur. J. Med. Chem.* 75 (2014) 282–288.
- [69] X. Nan, Y.F. Jiang, H.J. Li, J.H. Wang, Y.C. Wu, Design, synthesis and evaluation of sulfonylurea-containing 4-phenoxyquinolines as highly selective c-Met kinase inhibitors, *Bioorg. Med. Chem.* 27 (2019) 2801–2812.
- [70] Z.F. Zhang, J.C. Lee, L.P. Lin, V. Olivas, V. Au, T. LaFramboise, M. Abdel-Rahman, X.Q. Wang, A.D. Levine, J.K. Rho, Y.J. Choi, C.M. Choi, S.W. Kim, S.J. Jang, Y.S. Park, W.S. Kim, D.H. Lee, J.S. Lee, V.A. Miller, M. Arcila, M. Ladanyi, P. Moonsamy, C. Sawyers, T.J. Boggan, P.C. Ma, C. Costa, M. Taron, R. Rosell, B. Halmos, T.G. Bivona, Activation of the AXL kinase causes resistance to EGFR targeted therapy in lung cancer, *Nat. Genet.* 44 (2012) 852–860.
- [71] R. Tiedt, E. Degenkolbe, P. Furet, B.A. Appleton, S. Wagner, J. Schoepfer, E. Buck, D.A. Ruddy, J.E. Monahan, M.D. Jones, J. Blank, D. Haasen, P. Drueckes, M. Wartmann, C. McCarthy, W.R. Sellers, F. Hofmann, A drug resistance screen using a selective MET inhibitor reveals a spectrum of mutations that partially overlap with activating mutations found in cancer patients, *Canc. Res.* 71 (2011) 5255–5264.
- [72] T. Nakagawa, O. Tohyama, A. Yamaguchi, T. Matsushima, K. Takahashi, S. Funasaka, S. Shiratori, M. Asada, H. Obaishi, E7050: a dual c-Met and VEGFR-2 tyrosine kinase inhibitor promotes tumor regression and prolongs survival in mouse xenograft models, *Canc. Sci.* 101 (2010) 210–215.
- [73] L.B. Liu, A. Siegmund, N. Xi, P. Kaplan-Lefko, K. Rex, A. Chen, J. Lin, J. Moriguchi, L. Berry, L.Y. Huang, Y. Teffera, Y.J. Yang, Y.H. Zhang, S.F. Bellon, M. Lee, R. Shimanovich, A. Bak, C. Dominguez, M.H. Norman, J.C. Harmange, I. Dussault, T.S. Kim, Discovery of a potent, selective, and orally bioavailable c-Met inhibitor: 1-(2-Hydroxy-2-methylpropyl)-N-(5-(7-methoxyquinolin-4-yloxy)pyridin-2-yl)-5-methyl-3-oxo-2-phenyl-2,3-dihydro-1H-pyrazole-4-carboxamide (AMG 458), *J. Med. Chem.* 51 (2008) 3688–3691.
- [74] M.L. Peach, N. Tan, S.J. Choyke, A. Giubellino, G. Athauda, T.R. Burke Jr., M.C. Nicklaus, D.P. Bottaro, Directed discovery of agents targeting the Met tyrosine kinase domain by virtual screening, *J. Med. Chem.* 52 (2009) 943–951.
- [75] K.S. Kim, L.P. Zhang, R. Schmidt, Z.W. Cai, D. Wei, D.K. Williams, L.J. Lombardo, G.L. Trainor, D. Xie, Y.Q. Zhang, Y. An, J.S. Sack, J.S. Tokarski, C. Darienzo, A. Kamath, P. Marathe, Y.P. Zhang, J. Lippy, R. Jeyaseelan Sr., B. Wautlet, B. Henley, J. Gullo-Brown, V. Manne, J.T. Hunt, J. Fargnoli, R.M. Borzilleri, Discovery of pyrrolopyridine-pyridone based inhibitors of Met kinase: synthesis, X-ray crystallographic analysis, and biological activities, *J. Med. Chem.* 51 (2008) 5330–5341.